Zoological Journal of the Linnean Society, 2022, **XX**, 1–26. With 8 figures.

Call me by my name: unravelling the taxonomy of the gulper shark genus *Centrophorus* in the Mediterranean Sea through an integrated taxonomic approach

ANDREA BELLODI[†,1,2], ANNA BENVENUTO[†,2,3], RICCARDO MELIS[†,1,2], ANTONELLO MULAS[†,1,2], MONICA BARONE[4], CLAUDIO BARRÍA[5], ALESSIA CARIANI[*,2,3], LAURA CARUGATI[1,2], ARCHONTIA CHATZISPYROU[6], MONIQUE DESROCHERS[7], ALICE FERRARI[2,3], JAVIER GUALLART[8], FARID HEMIDA[9], CECILIA MANCUSI[10], CARLOTTA MAZZOLDI[11], SERGIO RAMÍREZ-AMARO[12], JAVIER REY[13], DANILO SCANNELLA[14], FABRIZIO SERENA[14], FAUSTO TINTI[2,3], ADRIANA VELLA[15], MARIA CRISTINA FOLLESA[1,2] and RITA CANNAS[*,1,2]

[1]*Department of Life and Environmental Sciences – University of Cagliari, Via T. Via Fiorelli 1, 09126 Cagliari, Italy*
[2]*CoNISMa Consorzio Nazionale Interuniversitario per le Scienze Mare, Piazzale Flaminio 9, 00196 Rome, Italy*
[3]*Department of Biological, Geological and Environmental Sciences – Alma Mater Studiorum University of Bologna, Via Sant'alberto 163, 48123 Ravenna, Italy*
[4]*Food and Agriculture Organization of the United Nations – Fisheries Division, Viale delle Terme di Caracalla, 00153 Rome, Italy*
[5]*Institut de Ciències del Mar, Passeig Marítim de la Barceloneta 37, 08003 Barcelona, Spain*
[6]*Hellenic Centre for Marine Research, Institute of Marine Biological Resources and Inland Waters, 576A Vouliagmenis Ave., 16452 Argyroupoli, Greece*
[7]*Northeastern University College of Science, 360 Huntington Ave, Boston, MA 02115, Massachusetts, USA*
[8]*Marine Biology Laboratory, Zoology Department, Universitat de València, Burjassot E-46100 València, Spain*
[9]*Ecole Nationale Supérieure des Sciences de la Mer et de l'Amenagement du Littoral, Dely Ibrahim 16320, Algiers, Algeria*
[10]*Environmental Protection Agency of Tuscany Region, Marine Division, Operational Unit Fisheries Resources and Marine Biodiversity, Via Marradi 114, 56127 Livorno, Italy*
[11]*University of Padova, Department of Biology, Via U. Bassi 58/B, 35131 Padova, Italy*
[12]*Instituto Español de Oceanografía, Centre Oceanogràfic de les Balears, Moll de Ponent s/n, 07015 Palma, Spain*
[13]*Instituto Español de Oceanografía, Centro Oceanográfico de Malaga, Muelle Pesquero s/n, 29640 Fuengirola, Spain*
[14]*Institute for Marine Biological Resources and Biotechnologies, National Research Council, Via Vaccara, 61, 91026, Mazara del Vallo, Italy*
[15]*Conservation Biology Research Group, Department of Biology, University of Malta, Msida, MSD2080, Malta*

Received 23 December 2020; revised 12 November 2021; accepted for publication 15 November 2021

*Corresponding authors. E-mail: rcannas@unica.it; alessia.cariani@unibo.it.
[†]These shared first authors contributed equally to this study.
[Version of record, published online 31 January 2022; http://zoobank.org/ urn:lsid:zoobank.org:pub:72E70407-171F-4ECC-A440-7AC6B72B5DCB]

The current shift of fishery efforts towards the deep sea is raising concern about the vulnerability of deep-water sharks, which are often poorly studied and characterized by problematic taxonomy. For instance, in the Mediterranean Sea the taxonomy of genus *Centrophorus* has not been clearly unravelled yet. Since proper identification of the species is fundamental for their correct assessment and management, this study aims at clarifying the taxonomy of this genus in the Mediterranean Basin through an integrated taxonomic approach. We analysed a total of 281 gulper sharks (*Centrophorus* spp.) collected from various Mediterranean, Atlantic and Indian Ocean waters. Molecular data obtained from cytochrome *c* oxidase subunit I (*COI*), 16S ribosomal RNA (16S), NADH dehydrogenase subunit 2 (*ND2*) and a portion of a nuclear 28S ribosomal DNA gene region (28S) have highlighted the presence of a unique mitochondrial clade in the Mediterranean Sea. The morphometric results confirmed these findings, supporting the presence of a unique and distinct morphological group comprising all Mediterranean individuals. The data strongly indicate the occurrence of a single *Centrophorus* species in the Mediterranean, ascribable to *C.* cf. *uyato*, and suggest the need for a revision of the systematics of the genus in the area.

ADDITIONAL KEYWORDS: deep sea – fisheries – phylogeny – shark fins – Squaliformes.

INTRODUCTION

The Mediterranean Sea is a marine biodiversity hotspot (Coll *et al.*, 2010). Among the numerous taxa inhabiting the basin, elasmobranchs play an important role, acting as apex predators with strong top-down effects on regulating the structure of marine communities (Dulvy *et al.*, 2008; Ferretti *et al.*, 2010). The global decline of coastal fish stocks over the last two centuries has led many industrial fisheries to expand their activities towards deeper, open-seas areas (Myers & Worm, 2003; Watson *et al.*, 2004; Morato *et al.*, 2006). This has also occurred in the Mediterranean Sea where, in the last century, commercial fisheries began to employ more sophisticated technologies and equipment, such as bottom trawls, gillnets and longlines to more effectively exploit less productive waters (Cartes *et al.*, 2004; Tudela, 2004; Pinello *et al.*, 2018). Unfortunately, these fishing practices represent the principal driving factor for bycatch of non-target fish such as sharks (Oliver *et al.*, 2015).

Deep-water sharks appear to be extremely vulnerable to fishing pressure and overexploitation due to their life-history traits, which include slow growth, longevity, late maturity and low fecundity (García *et al.*, 2008; Simpfendorfer & Kyne, 2009). Several authors have pointed out the high potential risk of extinction for deep-water sharks and have confirmed that information is still lacking on many of these species, related to both their biological characteristics and taxonomic resolution (Watson *et al.*, 2004; Morato *et al.*, 2006; García *et al.*, 2008; Simpfendorfer & Kyne, 2009).

Thus, the disentanglement of taxonomic uncertainties represents a fundamental step in the correct management of marine resources in general and specifically elasmobranchs, as shown by recent studies on *Squalus blainville* Risso, 1827 (Bellodi *et al.*, 2018) and *Raja polystigma* Regan, 1923 (Frodella *et al.*, 2016; Porcu *et al.*, 2020).

Among the elasmobranchs, *Centrophorus* Müller & Henle, 1837 (order Squaliformes: family Centrophoridae) is one of the genera with the most debated taxonomy (White *et al.*, 2017). This genus comprises a group of cosmopolitan deep-sea sharks inhabiting the benthopelagic waters of the outer continental shelves and upper continental slope between 50 and 2350 m deep from temperate to tropical waters across all oceans (Compagno, 1984; Ebert *et al.*, 2013; Veríssimo *et al.*, 2014). In the Mediterranean Basin, species of this genus always carry only one embryo per pregnancy, with gestation lasting up to 2–3 years, followed sometimes by a long resting period (Guallart, 1998; Guallart & Vicent, 2001). Over 30 nominal species have been recently considered valid in this genus (Ebert *et al.*, 2013; Veríssimo *et al.*, 2014), but its taxonomy has not been fully unravelled.

A global revision of the genus is still incomplete and is difficult due to the high degree of morphological similarity between several nominal taxa; therefore, the hard task of species discrimination is urgently needed. The original descriptions of the first species currently included in the genus are so poor that we are not sure that they actually describe a *Centrophorus*. In addition, several holotypes do not exist or could not be located, while others are incomplete and/or in poor condition, nullifying the comparison between original types of species and problematic specimens (Veríssimo *et al.*, 2014). Lastly, some morphological diagnostic characters may vary with ontogeny and, thus, in many cases, distinct ontogenetic stages of the same species may erroneously be considered as different species (Guallart *et al.*, 2013; White *et al.*, 2013, 2017; Veríssimo *et al.*, 2014). Add to this a long history of confusion, rectifications and mixing of data in the definition of characters have increased identification difficulties. On the whole, the lack of clear information from original descriptions and the absence of well-preserved holotypes have compromised the possibility to establish criteria to

clearly distinguish species with similar morphology and to assign them a correct species name (Guallart, 1998; Veríssimo *et al.*, 2014). This complication represents a limit for the correct identification of specimens with implications for species conservation and management purposes.

The studies performed in the last few years on species in the genus *Centrophorus* were aimed at clarifying the taxonomic ambiguities between some species (Guallart *et al.*, 2013; White *et al.*, 2013, 2017; Veríssimo *et al.*, 2014; Wienerroither *et al.*, 2015). The integration of molecular taxonomy techniques and traditional morphological analyses have allowed us to distinguish species that share a similar morphology, such as *Centrophorus granulosus* Bloch & Schneider, 1801 and *C. uyato* Rafinesque, 1810 (White *et al.*, 2013; Veríssimo *et al.*, 2014), previously discriminated mainly by their maximum size and size at sexual maturity. In the Atlantic Ocean and the Mediterranean Sea, these two nominal species were historically confused, either by using different names for the same species or using the same name for different species (Cadenat & Blache, 1981; Muñoz-Chapuli & Ramos, 1989).

In the Mediterranean, both *C. granulosus* and *C. uyato* have been reported regularly (Golani & Pisanty, 2000; Serena, 2005; Megalofonou & Chatzispyrou, 2006; Lteif *et al.*, 2017), and were both included in the Mediterranean shark species list by Serena (2005), following the precautionary principle. However, Veríssimo *et al.* (2014 and references therein) have suggested the occurrence of a single species in the basin. In addition, other recent studies, which employed molecular techniques for the identification of sharks in the Mediterranean, found a unique species of *Centrophorus*, reported as *C. uyato* (Vella *et al.*, 2017) or *C. granulosus* (Cariani *et al.*, 2017) and more recently as *C.* cf. *granulosus* (Leonetti *et al.*, 2020) or *C.* cf. *uyato* (Serena *et al.*, 2020).

The recent assessment of species diversity of Chondrichthyes in the Mediterranean Sea (Serena *et al.*, 2020) has suggested the possible occurrence of one valid species and has reiterated the need for taxonomic revision of the genus in the area since, to date, there is no comprehensive study resolving this taxonomic ambiguity. Most of the published works do not cover the entire basin and often employ either the morphological or the molecular method, but not both, to address this taxonomical problem. It has been widely demonstrated that the integration of both molecular and morphological methods for species identification is more effective to validate taxonomic assignment (Dayrat, 2005; White & Last, 2012; Ovenden *et al.*, 2013; Henderson *et al.*, 2016).

This study aims at clarifying the taxonomical issue regarding the genus *Centrophorus* in the Mediterranean Sea by combining both morphological and molecular methods. Samples were collected from different localities throughout the basin in order to obtain a representative coverage of the whole Mediterranean Sea. Sequenced data from three mitochondrial markers, cytochrome *c* oxidase subunit I (*COI*), 16S ribosomal RNA (16S) and NADH dehydrogenase subunit 2 (*ND2*), plus a portion of a nuclear 28S ribosomal DNA gene region (28S), were obtained and analysed to delineate discrete taxonomic units and to assess inter- and intraspecific genetic diversity and variability. Furthermore, traditional and landmark-based morphometry were employed to assess potential morphological differences and to provide useful diagnostic characters for the discrimination of species within the genus *Centrophorus*.

MATERIAL AND METHODS

Sampling

A wide network of collaborators was established to maximize the geographical coverage of the sampling and to collect a total of 281 samples of *Centrophorus* from different Mediterranean and Atlantic locations, representing 13 of the 27 Mediterranean General Fisheries Commission for the Mediterranean (GFCM) Geographic Sub Areas (GSA), including some African coastal areas (Fig. 1; Table 1; Supporting Information, Table S1). The sampling design covered three main areas of the Mediterranean Sea (western Mediterranean Sea, $N = 121$; central Mediterranean Sea, $N = 45$; eastern Mediterranean Sea, $N = 5$), and the central-eastern Atlantic ($N = 17$) and Indian Ocean ($N = 3$).

All specimens were collected between 2008 and 2019 during scientific surveys and commercial hauls. Photo vouchers were taken for morphological analyses using a digital camera and a table stand, when available. In each picture, specimens were arranged perpendicular to the camera on a uniformly coloured background to avoid distortions and a metric unit of measure was included. Morphological measurements were recorded from the obtained images following Compagno (2001) and Bellodi *et al.* (2018). When possible, sex and maturity stages were assessed according to the scales proposed for viviparous elasmobranchs (Follesa *et al.*, 2019a). Muscle tissue samples were collected and stored at –20 °C in 96% ethanol prior to the genetic analyses. Sampling information and other data associated with each specimen are presented in the Supporting Information, Table S1. Additionally, specimens and data collected were uploaded to the Barcode of Life Data system (BOLD, http://www.barcodinglife.org; Ratnasingham & Hebert, 2007).

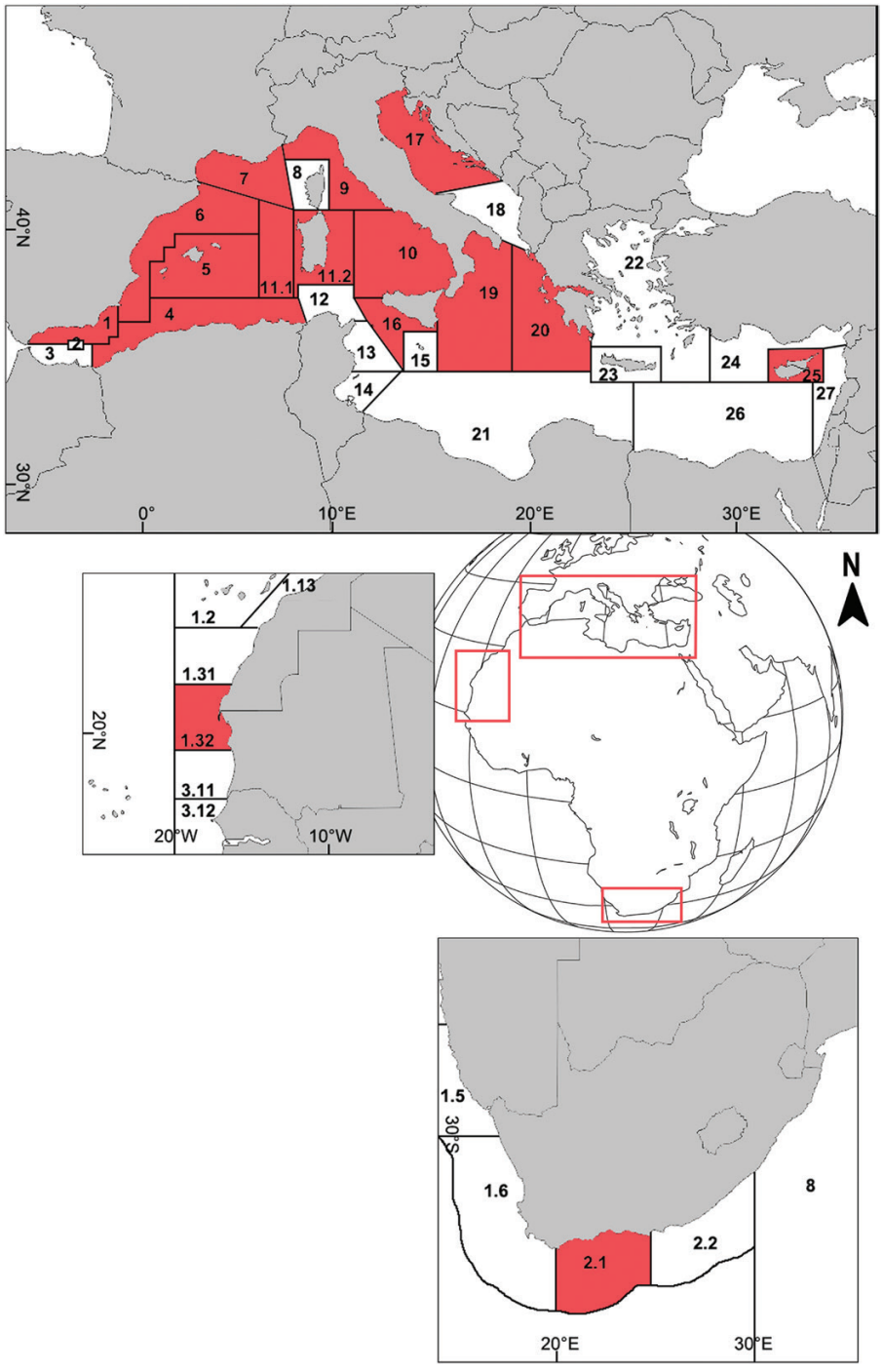

Figure 1. Map of Geographic Sub Areas and Food and Agriculture Organization (FAO) regions showing the sampling areas. Red colour highlights the geographical areas included in the sampling design.

MOLECULAR ANALYSIS

Details of the protocols used for DNA extraction, polymerase chain reaction (PCR) amplification and DNA sequencing of mitochondrial markers, are provided in the Supporting Information, Text S1.

The trace files obtained were checked and manually edited in MEGA v.X (Kumar *et al.*, 2016). Subsequently, the sequences were aligned using the ClustalW multiple sequence alignment algorithm (Thompson *et al.*, 1994). Mitochondrial coding gene sequences (*COI*

Table 1. Details of specimens sampled per area. *N* = total number of specimens collected per location. Field assigned species = field names for putative morphological species. The number of specimens assigned to each putative species is reported in brackets

Area	Location	*N*	Field assigned species
W Med	GSA 1	7	*Centrophorus* sp.
W Med	GSA 4	18	*C. granulosus* (14) *C. uyato* (4)
W Med	GSA 5	8	*Centrophorus* sp. (5) *C. granulosus* (3)
W Med	GSA 6	3	*Centrophorus* sp.
W Med	GSA 7	7	*Centrophorus* sp.
W Med	GSA 9	14	*C. granulosus*
W Med	GSA 10	4	*C. granulosus*
W Med	GSA 11	150	*C. granulosus*
C Med	GSA 16	24	*C. granulosus*
C Med	GSA 17	1	*C. uyato*
C Med	GSA 19	1	*C. granulosus*
E Med	GSA 20	19	*C. granulosus*
E Med	GSA 25	5	*C. granulosus*
CE Atlantic	FAO 34.1.32	17	*Centrophorus* sp. (2) *C. granulosus* (5) *C. squamosus* (10)
Indian	FAO 47.2.1	3	*C. squamosus*
TOTAL		281	

and *ND2*) were translated into protein sequences using MEGA, to check the presence of stop codons. Sequence data were uploaded to the BOLD system. Haplotypes for individual markers were retrieved using DnaSP v.6.12 (Rozas *et al.*, 2017) and deposited in GenBank (Accession numbers: 16S: OL671209 - OL671436; *COI*: OL670177 - OL670392; *ND2*: OL670514 - OL670727; 28S: OL670393 - OL670513).

Because the partition homogeneity test implemented in PAUP* v.4b10 (Swofford, 2002) indicated that the different fragments did not significantly differ in their phylogenetic signal (P = 0.98), the three mtDNA markers were analysed both separately and concatenated. The concatenation approach was used because of its presumed statistical advantages (Gadagkar *et al.*, 2005). The relationships among haplotypes were investigated using Haploviewer (Salzburger *et al.*, 2011).

The Mediterranean haplotypes were analysed using three approaches: neighbour-joining (henceforth NJ, implemented in MEGA), Bayesian inference (henceforth BI, using the MrBayes v.3.2.7 software; Ronquist *et al.*, 2012), and maximum likelihood method (henceforth ML, with PhyML; Guindon *et al.*, 2010). The support of the phylogenetic reconstruction was assessed with 1000 bootstrap replications (Felsenstein, 1985) for NJ and ML, and with 2 million iterations of the Markov chain Monte Carlo (MCMC) chains, with the first 25% of chains discarded as burn-in for the BI. The optimal evolutionary model was selected by the software jModelTest v.2.1.10 (Guindon & Gascuel, 2003; Darriba *et al.*, 2012) based on the corrected Akaike information criterion (AICc), and it was then employed for the analyses.

To estimate the occurrence of population structuring in the Mediterranean, the software ARLEQUIN v.3.5 (Excoffier & Lischer, 2010) was used for the analysis of molecular variance (AMOVA) using the TN93 model (Tamura & Nei, 1993) as the closest model implemented in ARLEQUIN to the HKY, which is the optimal evolutionary model identified by jModelTest.

For the *COI* sequences, barcodes index numbers (BIN) were generated automatically on BOLD using the 'refined single linkage (RESL) analysis'. This is a three-step algorithm that incorporates all available *COI* sequences and clusters them according to maximum values of intraspecific variation specific to orders and families (Ratnasingham & Hebert, 2013).

Additional sequences for the genus *Centrophorus* mined from online databases, such as BOLD and GenBank (http://www.ncbi.nlm.nih.gov/genbank/), were added to the alignments, including sequences from different species of the genus *Deania* Jordan & Snyder, 1902 used as outgroups for the phylogenetic tree construction (refer to the Supporting Information, Tables S2–S4 for sequence information). The names of taxa in the trees are in accordance with Fricke *et al.* (2021).

To assess the reliability of the sequences to discriminate among presumptive species, the so-called 'barcoding gap approach' was applied. The occurrence of a distinct gap between intraspecific and interspecific variability (Collins & Cruickshank, 2013) was checked by plotting the maximum intraspecific distance (MI) against the distance to the nearest neighbour (NN) for each putative species (Collins & Cruickshank, 2013); MI and NN distances were calculated using the

Kimura's two-parameter (K2P; Kimura, 1980) model with the R package SPIDER v.1.5 (Brown *et al.*, 2012). Principal coordinates analysis (PCoA) was performed with SPIDER based on the K2P genetic distance matrix using the function ordinDNA().

Considering that BIN cannot be obtained for sequences other than *COI* in BOLD and given that the 2.2% threshold used by BOLD (Ratnasingham & Hebert, 2013) is often not the most appropriate threshold for every reference dataset, especially when there are unsampled species, identification success can be increased if a better threshold is used (Meyer & Paulay, 2005). Here, we used the function threshOpt() implemented in SPIDER to perform this analysis, following the author's tutorial indications (Brown & Collins, 2011). The function returned the number of true-positive, false-negative, false-positive and true-negative identifications at a given threshold, and it allowed us to calculate the optimum threshold value that minimizes errors (FP, the false-positive-no conspecific matches within threshold of query and FN, false-negative identifications-non-conspecific species within threshold distance of query, i.e. the cumulative error). Once the optimal threshold had been identified, it was used with the species delimitation method 'best close match analysis' (henceforth BCMA, Meier *et al.*, 2006) performed in SPIDER. BCMA is slightly different from the RESL method because it only operates upon the single nearest-neighbour match, rather than on all matches within the threshold (Brown & Collins, 2011). To perform the BCMA, sequences were provisionally attributed to different putative molecular operational taxonomic units (MOTU) based on their morphological features, their placement in highly supported branches in the trees and/or the BIN attribution by BOLD (for the *COI* sequences only).

As an alternative to the 'distance-based' approach, the 'character-based' DNA barcoding approach was also used, in which species are identified through the presence or absence of discrete nucleotide substitutions (character states) within a DNA sequence (Rach *et al.*, 2008). The list of private diagnostic nucleotides for each species (i.e. those nucleotides that are fixed within species and different from all other species) was obtained using SPIDER's function 'nucDiag' based on the procedure described in Sarkar *et al.* (2008). They can be used as diagnostic characters that allow for unambiguous identification of species or diagnostic entities.

Morphological measures and geometric morphometrics

Because most of the available sample images were lateral, traditional morphometric analyses were first performed considering 28 somatic measurements, including the 21 measurements described as a discriminant for species identification in the genus *Centrophorus* by Veríssimo *et al.* (2014). Measurements were taken using the free software tpsDig2 v.2.31 (Rohlf, 2015). For each digitized picture, a scale factor was set employing the unit of the measure included in the picture. All measurements were expressed in centimetres, and names and abbreviations were defined according to Veríssimo *et al.* (2014; Supporting Information, Fig. S1). Raw measurements for each individual were expressed in percentages of total length (TL). Total length was defined as the distance between snout tip and the projection of the caudal fin posterior margin when in a natural position. On the contrary, other characters suggested by recent publications (White *et al.*, 2013, 2017; Veríssimo *et al.*, 2014), such as dermal denticles and teeth shape, were not used in this study, because the only material available from many areas was comprised of photos of the entire body and it was impossible to directly inspect most of the specimens. A specific a priori hypothesis was defined before computing the similarity matrix based on the Euclidean distance. We hypothesized that the different species of *Centrophorus* were characterized by different morphological parameters. Therefore, all specimens were classified according to the molecular assignment when available. Once the hypothesis was established, a canonical analysis of principal coordinates (CAP) routine was performed with the PRIMER v.7 software (Clarke & Gorley, 2015) on the similarity matrices previously computed to test the hypothesis. The CAP analysis resulted in a plot representing groups of multivariate points by reference to a predetermined a priori hypothesis and in cross-validation confirming or not the a priori classification of species. Using the same software, a SIMilarity PERcentages (SIMPER) analysis was performed to investigate which morphometric measurements were most responsible for the definition of the groups. An additional 49 Mediterranean individuals without any molecular data were also available. For this reason, their a priori classification was impossible and hence they were excluded from the main analysis. However, they were morphologically identified a posteriori by checking their distribution in a secondary CAP scatterplot.

We integrated traditional morphometric analyses with geometric morphometry to investigate in-depth the morphological variation in the Mediterranean samples of *Centrophorus*. Landmarks-based techniques, being based on shape instead of linear measurements, allowed us to highlight different sources of phenotypic variation among species (Schmieder *et al.*, 2015; Guillaud *et al.*, 2016; Wilke *et al.*, 2016; Boroni *et al.*, 2017; Ibáñez & Jawad, 2018).

Geometric morphometric analyses were undertaken on the first and the second dorsal and on the caudal fins (D1, D2 and C, respectively), because

these structures are stiff enough to maintain their shape in dead specimens and also because of their functional importance. A total of 105 caudal fins, 46 first dorsal fins and 50 second dorsal fins were considered appropriate for this analysis from the pool of specimens sampled. The selection of landmarks on these structures was relatively straightforward because of their fundamental two-dimensionality.

TPS files were created to store all usable images using tpsUtil v.1.76 (Rohlf, 2015). For each specimen and structure, five landmarks were positioned on D1 and D2, while seven landmarks were positioned on C (Supporting Information, Fig. S2). All landmarks were digitized using tpsDig2 v.2.31 (Rohlf, 2015). For each specimen, landmarks were positioned twice to reduce possible positioning errors. Using the software MorphoJ v.1.06 (Klingenberg, 2011), the average of the two measurements was computed. The resulting coordinates were analysed with MorphoJ after a Procrustes transformation (Rohlf, 1999). The Procrustes transformation rotates, translates and scales all images to obtain a final superimposed image that allows the comparison of all landmark configurations. The repeatability of the landmark was checked through a scatterplot, and a covariance matrix was then generated.

Principal component analysis (PCA) was performed with MorphoJ to visualize the interindividual variation of each structure (D1, D2 and C) in the set of samples. Procrustes ANOVA tests were conducted to investigate significant differences in terms of shape and size of the centroid among species. The differences among taxa were also investigated using canonical variates analysis (CVA) which maximizes the separation between the groups (species in this case) defined a priori according to the genetic hypothesis. A permutation test of 10 000 replications was employed to determine the statistical significance of pairwise differences using Procrustes distances. Finally, the percentage of classification/misclassification was calculated through a discriminant function analysis (DFA) computed on 10 000 permutations between the pairs of groups (putative species) defined a priori. To evaluate the occurrence of sex-based and ontogenetic morphological variation, intraspecific analyses were performed on a subset of samples. Intraspecific differences between sexes were investigated through PCAs and Procrustes ANOVAs. Furthermore, two regression models were performed plotting the centroid size and the shape scores against the TL of the specimen to verify the presence of allometry.

RESULTS

New sequence data

The collaborative research network enabled the implementation of the BOLD dataset '*Gulper sharks in the Mediterranean Sea*' (Code DS-GULPMED), which currently includes a total of 232 specimens. All specimens have been successfully processed for DNA extraction, but some failed to provide sequence data for one or several fragments. Details of the individuals sequenced are summarized in the Supporting Information, Table S1.

A total of 208 individuals have been successfully sequenced for the three mitochondrial fragments. The *ND2* fragment is the most variable with a total of 34 haplotypes, whereas *COI* and 16S sequences revealed 13 haplotypes each. Final alignment of 2146 bp was obtained by concatenating the sequences (16S: 527 bp, *COI*: 588 bp and *ND2*: 1031 bp), for a total of 54 haplotypes (Supporting Information, Table S5). The networks for the single markers (data not shown) and for the concatenated sequences (Fig. 2) show the occurrence of three groups of haplotypes, separated by tens of mutations, corresponding to three putative distinct species. The largest group of haplotypes, Group 1, encompasses 38 out of 54 haplotypes derived from all Mediterranean sharks and four individuals caught in Mauritania (CE Atlantic). Within this group, the analysis highlights the occurrence of a principal haplotype (H1), which is shared among 66 sequences (32%) from all the locations, except from the Atlantic samples, which have private haplotypes. In the Mediterranean, several other private haplotypes are present, as well as shared haplotypes among western, central and eastern locations, without any clear geographical segregation. The AMOVA confirms the lack of structure (genetic differentiation) both overall ($\Phi = 0.003$, $P = 0.4$) and among the Mediterranean sub-basins ($\Phi = 0.008$, $P = 0.4$).

The second and the third group of haplotypes have been found only in Mauritania (Group 2), and in Mauritania + South Africa (Group 3). Within the three groups, there is little variability (from 0.09 to 0.22% nucleotide site differences), while the differences among groups are higher (range 3.4-4.4% site differences), with the distance between Groups 1 and 2 being the highest. The optimal evolutionary model HKY+I+G (p-inv = 0.72, gamma shape = 0.63; Hasegawa *et al.*, 1985) was used to build the evolutionary trees. The NJ, ML and BI highlight the occurrence of three monophyletic clades supported by 99–100% bootstrap and posterior probabilities values (data not shown). The nuclear 28S sequences have been initially amplified in a subset of samples ($N = 127$) and show low variability: a total of 3 bp differences out of a total of 304 bp. They allow us to identify the three groups, with 2 bp fixed differences among them and no variability within them. Given their scarce informative power, 28S sequence data have not been obtained for the whole dataset.

From a molecular point of view, groups are clearly differentiated. Nevertheless, Groups 1 and 2 contain

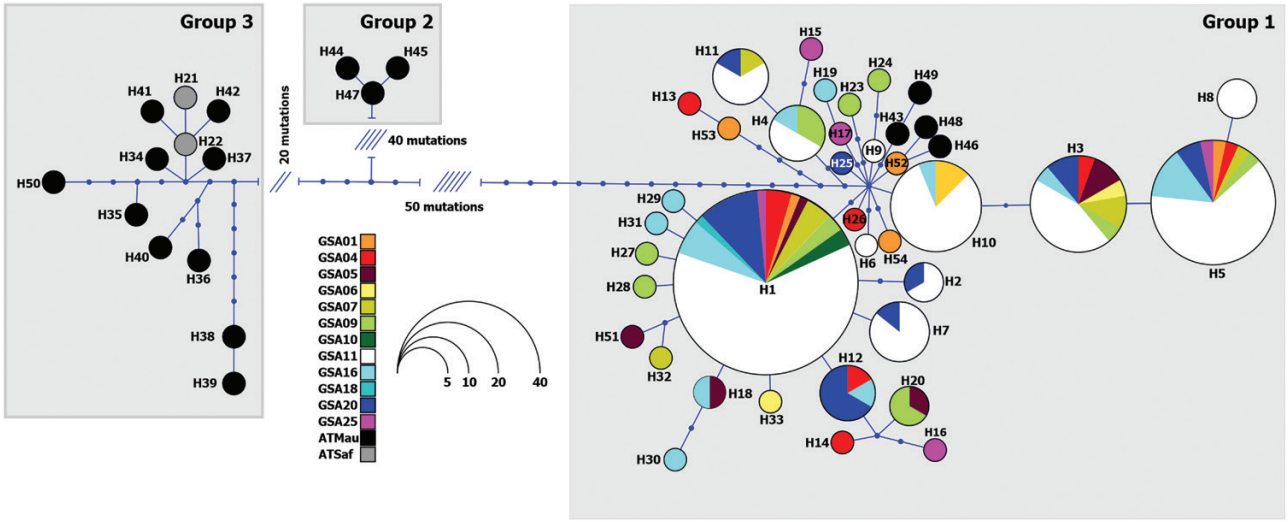

Figure 2. Median joining network of the haplotypes for the concatenated fragments. The circle size is proportional to the frequency of each haplotype, the segments represent one mutational event.

specimens assigned in the field to different putative morphological species (*C. granulosus*, *Centrophorus* sp. and *C. uyato*; see Supporting Information, Table S1), while Group 3 contains only specimens 'morphologically' assigned to *Centrophorus squamosus* Bonnaterre, 1788. To resolve this uncertainty, our sequences have been compared with public sequences mined from GenBank and BOLD.

Comparisons with deposited public sequences

Unfortunately, the three fragments used in this study had never been obtained together for any specimen previously analysed, therefore our sequences could only be compared with the public sequences as single fragments and not as concatenated sequences. Here, a total of 224, 228 and 214 sequences have been obtained for *COI*, 16S and *ND2*, respectively (Supporting Information, Tables S2–S4). They have been added to the homologous sequences deposited for the genera *Centrophorus* and *Deania* in public sequence repositories, for a total of 555 *COI* (560 bp long; 90 haplotypes), 259 *ND2* (1027 bp; 60 haplotypes) and 274 16S (502 bp; 30 haplotypes) sequences. For all three genes, the barcode gap exists for each species, meaning that the genetic distance between each conspecific individual was smaller than to any allospecific individual (Fig. 3). This gap is wider in *ND2*, followed by *COI* and narrow for the 16S sequences; these differences are clearly visible in the PCoA plots (Supporting Information, Fig. S3).

Concerning *COI* sequences, among the sequences deposited as *Centrophorus* or *Deania* (family Centrophoridae), some are notably divergent and belong to two different shark families (Squalidae and Etmopteridae); they have been used as outgroups to root the trees. Excluding the outgroups, the BOLD system assigned *COI* sequences to 14 BINs, ten of which were for the genus *Centrophorus*. Concordantly, the NJ, ML and BI trees clustered 208 out of 224 of our sequences in a strongly supported clade identified by the BOLD system as BIN AAB4327, ascribable to Clade A *sensu* Veríssimo *et al.* (2014) and corresponding to Group 1 of the concatenated sequences. In this same clade, an additional 99 sequences (ten haplotypes) have been found from specimens collected in a wide geographical range, encompassing the whole Mediterranean Sea and almost all oceans (Atlantic, Indian and Pacific Oceans; for details see Fig. 4 and the Supporting Information, Table S2 and Figs S4, S5). Also, 13 of our *COI* sequences clustered in a strongly supported monophyletic clade identified by the BOLD system as BIN AAB6688, ascribable to Clade E *sensu* Veríssimo *et al.* (2014) and corresponding to Group 3 of the concatenated sequences (Fig. 4; Supporting Information, Figs S4, S5). In this same clade, 36 other sequences (12 haplotypes) are placed from specimens collected in three oceans (Atlantic, Indian and Pacific Oceans) and only one sampled in the most western part of the Mediterranean (Algeria; Table S2). The remaining three of our *COI* sequences clustered in a strongly supported clade identified by the BOLD system as BIN ABZ3018, ascribable to Clade D *sensu* Veríssimo *et al.* (2014) and corresponding to Group 2 of the concatenated sequences (Fig. 4; Supporting Information, Figs S4, S5). In this same clade, another 48 sequences (ten haplotypes) have been found belonging to specimens collected in three oceans (Atlantic, Indian and Pacific Oceans), but not in the Mediterranean Sea (Supporting Information, Table S2). Following

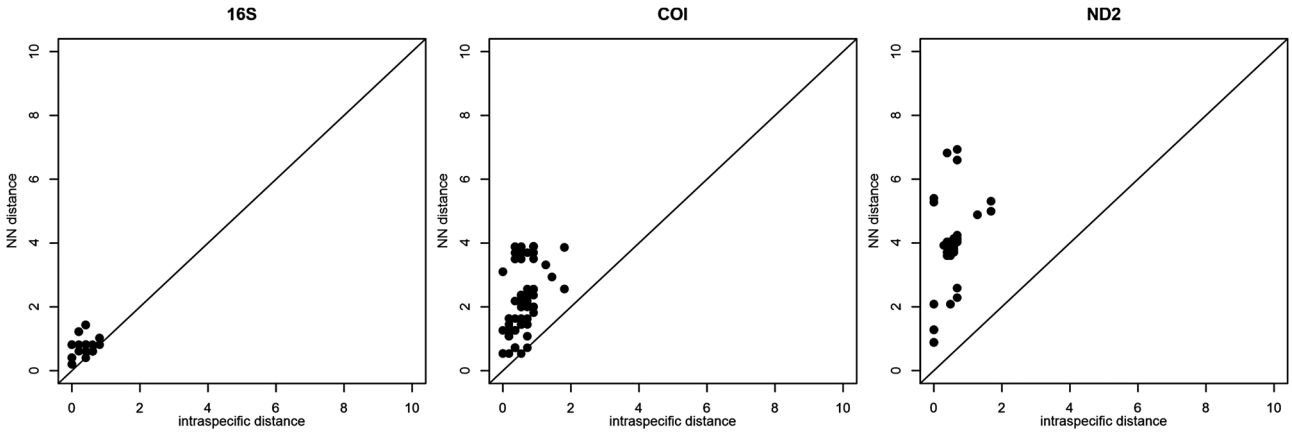

Figure 3. Comparison of NN (nearest neighbour or minimum interspecific distance) and maximum intraspecific distances for the different gene fragments. Equal intra- and interspecific variation is marked by the diagonal line. Points above the diagonal indicate 'species' with 'barcode gaps'.

the nomenclature adopted by Veríssimo *et al.* (2014) and White *et al.* (2013, 2017), specimens in Clades A, D and E are attributed to the nominal species *C.* cf. *uyato*, *C. granulosus* and *C. squamosus*, respectively. A unique BIN (ACS4629) has been assigned to Clade B *sensu* Veríssimo *et al.* (2014), even if the sequences are clustered in two distinct, well-supported lineages, corresponding to two distinct species: the newly described *Centrophorus leislei* White *et al.*, 2017 and the still undescribed *Centrophorus* sp. 1 from the Gulf of Mexico (Veríssimo *et al.*, 2014). Similarly, Clade C *sensu* Veríssimo *et al.* (2014) corresponds to a single BIN (AAB4328), but contained two close species of long-snouted gulper sharks, *Centrophorus harrissoni* McCulloch, 1915 and *Centrophorus isodon* Chu *et al.*, 1981. The opposite is true for Clade E, in which two BINs were assigned to sequences that in the trees appear in the same lineage, and for Clade H in which separate BINs cluster together. Finally, sequences from *Deania quadrispinosa* McCulloch, 1915 appear in two well-supported branches (Clades L and M), assigned to two BINs, suggesting the possible occurrence of cryptic taxa.

According to the BCMA analysis, the optimal threshold estimation for *COI* sequences results in a nucleotide distance value of 0.5%, with an associated cumulative error of three (FN = 0; FP = 3). Using this threshold, BCMA results confirm that, despite being assigned to two BINs, $MOTU_7$ (originally classified as *C.* cf. *squamosus*) is indistinguishable from $MOTU_6$ (*C. squamosus*) in Clade E, the same for $MOTU_9$ (*C.* cf. *isodon*) and $MOTU_{10}$ (*C. harrissoni*) in C, and $MOTU_{16}$/$MOTU_{17}$ in Clade H (*Centrophorus atromarginatus* Garman, 1913).

Similar results have been obtained with the 16S sequences in which our sequences cluster in three distinct well-supported clades: all our Mediterranean sequences are together in the abovementioned Clade A of Veríssimo *et al.* (2014), the South African sequences in Clade E, whereas the sequences from Mauritania are found in the three different clades: Clades A, D and E (Fig. 5; Supporting Information, Figs S6, S7).

The optimal threshold identified through the BCMA analysis for the 16S sequences resulted in a nucleotide distance value of 0.4%, with an associated cumulative error of four (FN = 0; FP = 4). Using this threshold, all the MOTUs corresponding to morphologically described species are recognized, except for $MOTU_2$ (originally deposited as *Centrophorus lusitanicus* Barbosa du Bocage & de Brito Capello, 1864), which is indistinguishable from $MOTU_1$ (*C. squamosus*), and $MOTU_3$ (haplotype shared between *C. isodon* and *harrissoni*), which is indistinguishable from $MOTU_4$ (*Centrophorus* sp. 1).

ND2 provides similar outputs: our sequences cluster in three well-supported clades (Fig. 6; Supporting Information, Figs S8, S9), along with *ND2* sequences from specimens attributed to *C. uyato*, 'true' *C. granulosus* and *C. squamosus* by White *et al.* (2017). The optimal threshold identified through the BCMA analysis for *ND2* sequences, resulted in a nucleotide distance value of 0.8%, with an associated cumulative error of zero (FN = 0; FP = 0), meaning that all MOTUs shown in Figure 6 are recognized as separate, indicating a possible subdivision of *Centrophorus longipinnis* White *et al.*, 2017 and *D. quadrispinosa*.

Diagnostic characters

In the Supporting Information, Table S6 shows the diagnostic character states of the investigated gene regions. In general, many molecular diagnostic characters are found when only our newly generated sequences are used. The highest number of diagnostic

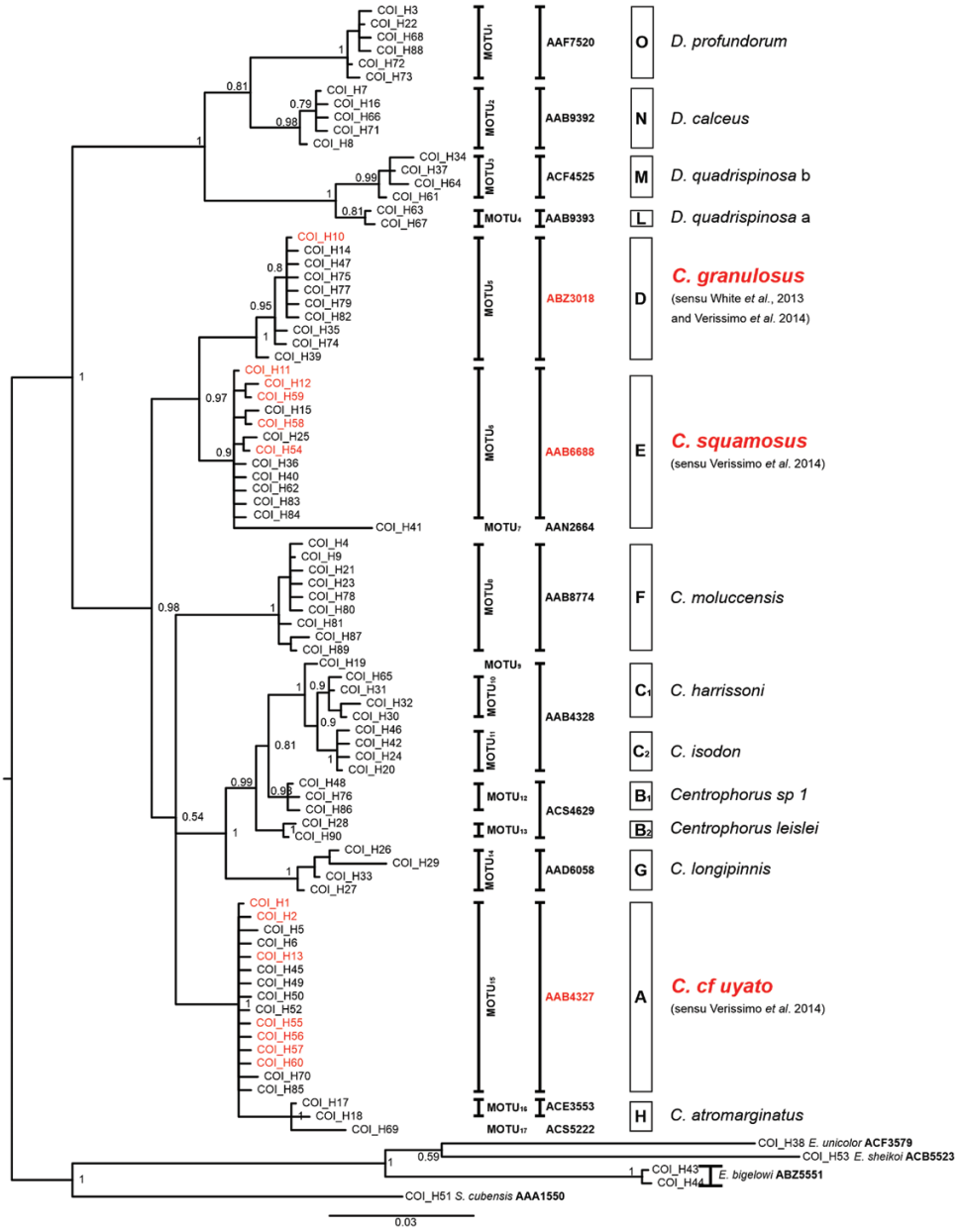

Figure 4. Bayesian phylogenetic tree of the *COI* haplotypes. Near the nodes are the support values, shown as posterior probability. In red the haplotypes from individuals sequenced in the present study. On the right of the tree, the assigned OTU, the BIN, the clade identified by the BCMA analysis, as well as the putative nominal species are indicated.

characters was found for *ND2* and the lowest for 28S, but in any case, the clear discrimination of the three species of Centrophoridae under investigation can be achieved through a character-based DNA barcoding approach. When shortening these sequences to include additional public sequences and species in the analyses, the number of diagnostic characters decreases. Species-specific sites are always identified in *ND2*, while *COI* and 16S fail to provide suitable diagnostic characters for a few taxa (Supporting Information, Table S7).

MORPHOMETRIC ASSESSMENT

A matrix of 122 specimens with 28 body measurements expressed in %TL (Supporting Information, Table S8) was obtained for morphometric analyses. The 122 specimens have been a priori classified according to the molecular results as follows: 109 samples as *C.* cf. *uyato*, ten as *C. squamosus* and three as *C. granulosus*.

The plot obtained from the CAP analysis shows clear segregation among *C.* cf. *uyato* and *C. squamosus* groups, whereas the specimens classified as

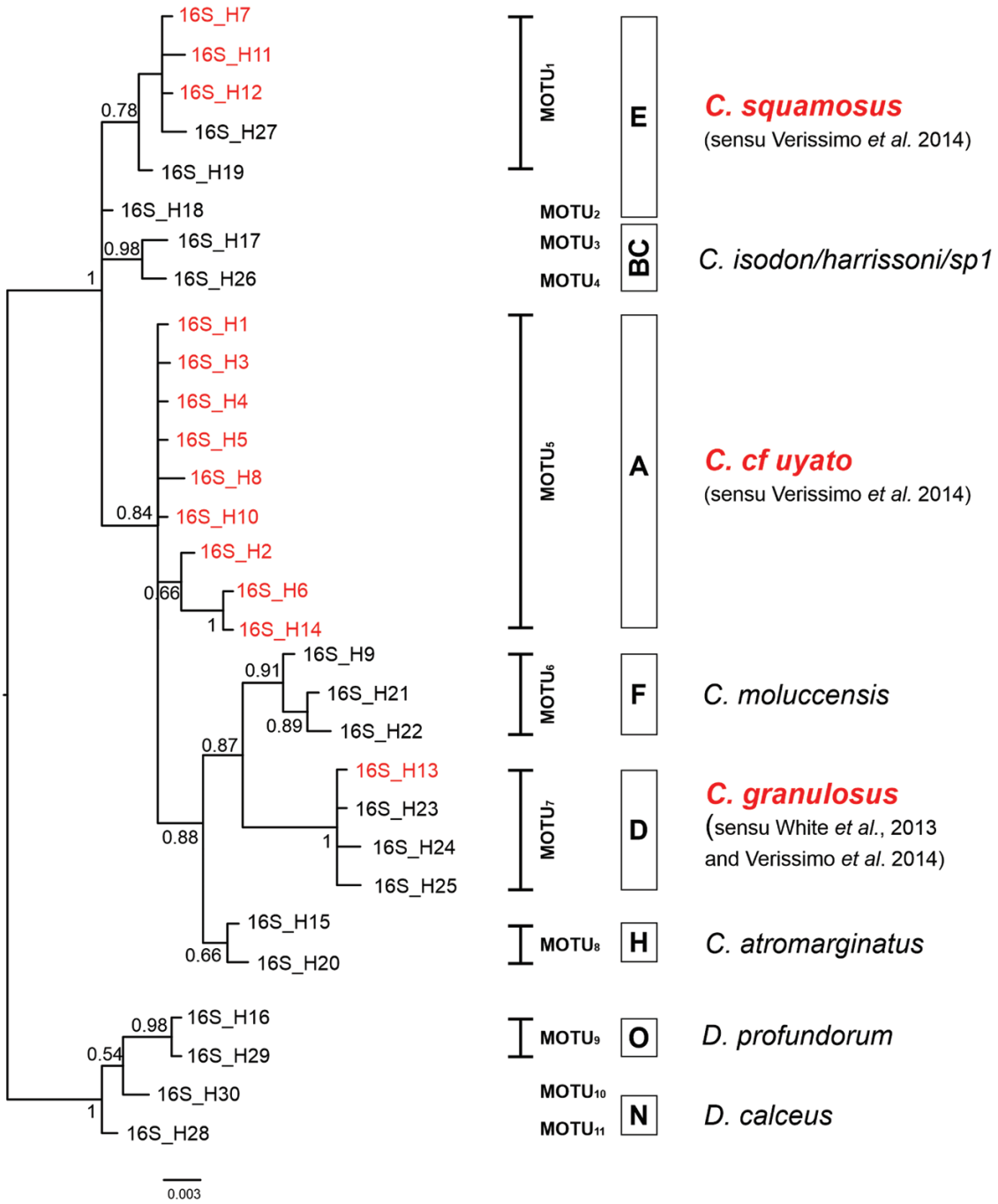

Figure 5. Bayesian phylogenetic tree of the 16S haplotypes. Near the nodes are the support values, shown as posterior probability. In red the haplotypes from individuals sequenced in the present study. On the right of the tree the assigned OTU and the clade identified by the BCMA analysis, as well as the putative nominal species are indicated.

C. granulosus lay in between (Fig. 7). The *C.* cf. *uyato* specimens caught in Atlantic waters are slightly displaced from the main group, with their data points located at the margin of the cloud, oriented towards the other species groups (Fig. 7). The cross-validation confirms the graphic output, reporting a high percentage of correct assignment of 96.7% (118/122). Consequently, only four individuals out of 122 have been misclassified (3.3%; Supporting Information, Table S9). Among groups, all ten *C. squamosus* specimens are always correctly identified, while only two of 109 specimens a priori classified as *C.* cf. *uyato* have been attributed

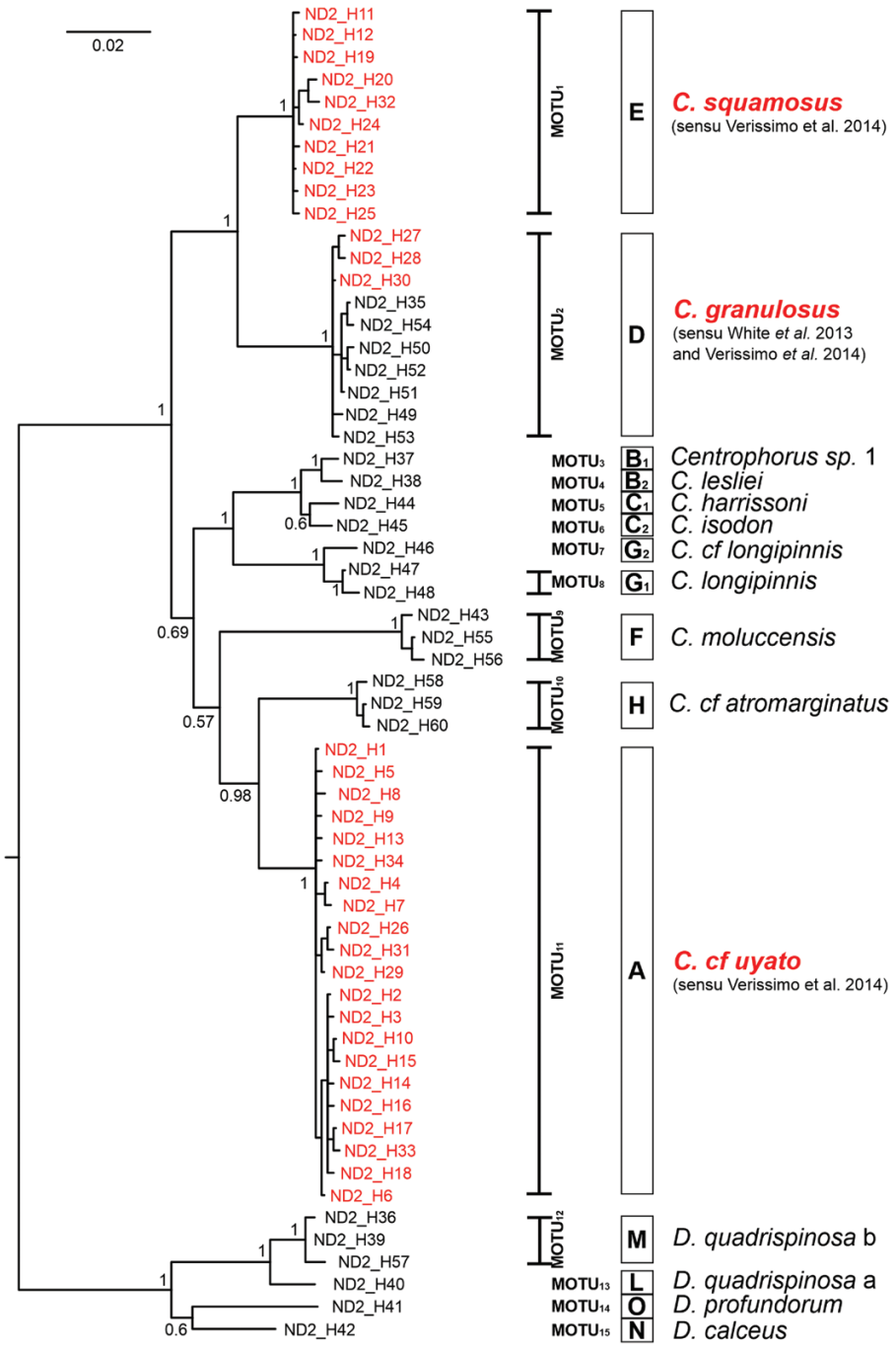

Figure 6. Bayesian phylogenetic tree of the *ND2* haplotypes. Near the nodes are the support values, shown as posterior probability. In red the haplotypes from individuals sequenced in the present study. On the right of the tree the assigned OTU and the clade identified by the BCMA analysis, as well as the putative nominal species are indicated.

to *C. granulosus*. The highest misidentification rates are found in the *C. granulosus* group, where two of the three individuals are misclassified as *C.* cf. *uyato* and only one is correctly grouped.

The SIMPER analysis at intraspecific level reveals that about 50% of the average group similarity is due to the same eight body-length measurements, and in the same order of importance: FL, PD2, PP2, PD1, IDS, HDL, PG1 and CDM, with the only exception of *C.* cf. *uyato* in which PG1 and CDM are inverted (Supporting Information, Table S10). For each shark group, the mean values of the measurements (± SD) are reported

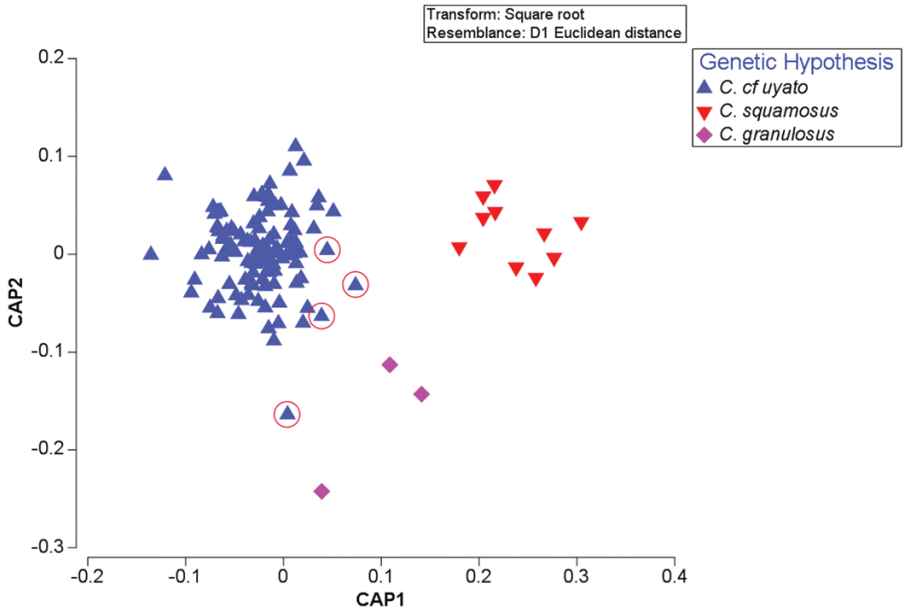

Figure 7. Analysis of principal coordinates (CAP) scatterplot representing the morphometric differences observed among the species classified as a result of the genetic analyses. Specimens of *Centrophorus* cf. *uyato* collected in the Atlantic Ocean are circled in red.

in Table 2. A secondary CAP analysis, computed to morphologically identify the further 49 Mediterranean individuals without molecular data, displayed an overlapping distribution of these specimens with the other Mediterranean samples classified as *C.* cf. *uyato* (Supporting Information, Fig. S10; Tables S8, S9).

The most important measurement responsible for interspecific differences is the pectoral fin inner margin (P1I), which appears as the major factor in discriminating *C. squamosus* from the other groups (SIMPER Contrib% = 13.45 and 11.02 with *C.* cf. *uyato* and *C. granulosus*, respectively) (Supporting Information, Table S10). Concerning other measurements that contribute to the observed differences among groups, the scenario is various, with several different measurements contributing with similar percentages (Supporting Information, Table S10). The D1 Base (D1B: SIMPER Contrib% = 6.00) is the main source of difference between the *C.* cf. *uyato* and *C. granulosus* groups, followed by two body length measurements: fork length (FL: SIMPER Contrib% = 5.91) and pre-pelvic length (PP2: SIMPER Contrib% = 5.01; Supporting Information, Table S10).

In relation to the geometric morphometric analyses carried out on the three structures (C caudal fin, D1 first dorsal and D2 second dorsal), the PCAs performed show that the first two components account, respectively, for 62.77%, 71.57% and 73.59% of the variance, whereas the amount of variance explained by the first three components is 77.96%, 87.23% and 86.77%, respectively (Fig. 8).

When comparing the measurements of the caudal fins, the Procrustes ANOVA highlighted significant differences among species in terms of shape ($P < 0.001$), but no difference in the size of the centroid. On the contrary, the same analysis performed on the dorsal fins showed significant interspecific differences both in terms of centroid size and shape for the first ($P = 0.006$; $P < 0.001$) and the second dorsal fins ($P = 0.013$; $P < 0.001$).

Intraspecific analyses have been performed on a subset sample of 93 caudal fins, 37 first dorsal fins and 41 second dorsal fins belonging to specimens molecularly identified as *C.* cf. *uyato*. In the three PCAs performed, the first two components account for the 64.22%, 63.44% and 69.20% of variance, whereas the first three components explain the 79.99%, 84.79% and 86.36% of variance, respectively (Supporting Information, Fig. S11).

Procrustes ANOVAs performed on the three fins did not show any significant differences in terms of both centroid size and shape between the sexes ($P > 0.05$). The CVA plots obtained for C, D1 and D2 showed a clear separation of *C. squamosus* from the other groups and a subtler differentiation between *C.* cf. *uyato* and *C. granulosus* (Supporting Information, Fig. S12). Procrustes distances among the groups were significantly different in the pairwise comparisons between *C. squamosus* and both *C.* cf. *uyato* and *C. granulosus* ($P < 0.05$), but not for those between *C.* cf. *uyato* and *C. granulosus*. These results were, in part, confirmed by the discriminant function outputs

Table 2. Mean values (± SD) of the eight body length measurements that, according to the SIMPER analysis, contribute to the most intraspecific variability for each shark group. Nomenclature and abbreviations were defined according to Veríssimo *et al.* (2014): FL, fork length; PD2, pre-second dorsal fin length; PP2, pre-pelvic fin length; PD1, pre-first dorsal fin length; IDS, inter-dorsal space, defined as 'Distance from first dorsal fin insertion to second dorsal fin insertion'; HDL, head length; PG1, pre-branchial length; CDM, dorsal caudal fin margin; P1I, pectoral fin inner margin. Further details on the measurements in the main text and Figure S1.

	FL		PD2		PP2		PD1		IDS		HDL		PG1		CDM		P1I	
Group	mean	SD	mean	SD	mean	SD	mean	SD	mean	SD	mean	SD	mean	SD	mean	SD	mean	SD
C. cf. uyato	91.12	3.41	69.72	3.18	62.90	4.51	32.89	1.91	31.28	3.79	21.93	2.31	17.23	2.27	17.88	1.71	13.57	2.85
C. granulosus	84.03	12.28	65.41	7.94	60.12	8.04	29.47	2.55	29.65	3.37	21.51	3.24	15.96	2.43	15.86	2.81	12.94	1.01
C. squamosus	90.91	1.76	69.22	1.73	65.10	2.02	31.99	1.42	31.47	1.69	21.92	2.00	16.62	1.68	16.12	1.53	7.13	1.96

Figure 8. Principal component analysis (PCA) conducted on caudal fin (A), first dorsal fin (B) and second dorsal fin (C) landmarks. Blue, pink and red dots represent, respectively, *Centrophorus* cf. *uyato*, *Centrophorus granulosus* and *Centrophorus squamosus* samples.

reporting significant differences ($P < 0.05$) in Procrustes distance means computed between *C.* cf. *uyato* and *C. granulosus* and *C.* cf. *uyato* and *C. squamosus* for what concerns C, and between *C.* cf. *uyato* and *C. squamosus* and *C. granulosus* and *C. squamosus* for D1 and D2. In all other pairwise comparisons, the difference was not significant. According to the shape of C, D1 and D2, samples were correctly classified in their species 95.7%, 86.5% and 85% of the time for *C.* cf. *uyato*, 83.3%, 100% and 75% for *C. granulosus* and 94.4%, 100% and 100% for *C. squamosus* respectively (Supporting Information, Table S11).

The regression models performed to verify the presence of ontogenetic allometry showed a significant relationship between the centroid size and the TL, both for the caudal ($P < 0.001$; $r^2 = 0.87$) and for the first ($P < 0.001$; $r^2 = 0.81$) and the second dorsal fins ($P < 0.001$; $r^2 = 0.69$) (Supporting Information, Fig. S13). The relation between the shape and the TL was significant for the caudal ($P < 0.001$; $r^2 = 0.25$), the first dorsal (P-value = 0.009; $r^2 = 0.92$) and the second dorsal fins as well (P-value = 0.0001; $r^2 = 0.20$) (Supporting Information, Fig. S14).

DISCUSSION

The present study was conceived to clarify the taxonomic uncertainty associated with the genus *Centrophorus* throughout the Mediterranean Sea, integrating molecular and morphological methods.

New genetic data for *Centrophorus* in the Mediterranean Sea

The present work complements the ELASMOMED DNA barcode reference library for chondrichthyans in the Mediterranean Sea compiled by Cariani *et al.* (2017). Regarding species of *Centrophorus*, the library was based only on 12 sequences from individuals caught in four areas (Sardinia, Algeria, Sicily and the Ionian Sea), whereas here the new DNA data cover the whole basin, with an additional nine Mediterranean GSAs and some new locations in the Atlantic (Mauritania) and Indian Oceans (South Africa). More Mediterranean sequences, retrieved from former studies [Malta: GSA15 in Vella *et al.* (2017)] and public repositories (Israel: GSA27, unpublished sequences; see Supporting Information, Tables S2–S4 for details), were analysed and compared. Moreover, DNA barcodes were obtained not only for the *COI* sequences, but also for three additional genes (two mitochondrial, the 16S and *ND2*, and the nuclear 28S) to capture as much genetic variation as possible in the area and to increase the resolutive power of the genetic data. Previous studies mainly used a single marker, *COI* (Ward *et al.*, 2005, 2008; Moura *et al.*, 2008, 2015; Wong *et al.*, 2009; Costa *et al.*, 2012; Sanjuán *et al.*, 2012; Wienerroither *et al.*, 2015; Chuang *et al.*, 2016; Bineesh *et al.*, 2017; Cariani *et al.*, 2017; Rodríguez-Cabello *et al.*, 2020), 16S (Douady *et al.*, 2003; Daley *et al.*, 2012) or *ND2* (Naylor *et al.*, 2012a, b; Straube *et al.*, 2013; White *et al.*, 2013, 2017; Fernando *et al.*, 2019). In a few cases 16S + *COI* (Straube *et al.*, 2010; Veríssimo *et al.*, 2014) or *COI* + *ND2* data (Vella *et al.*, 2017; Ramírez-Amaro *et al.*, 2018) were combined. Sequenced data for 28S are obtained for the first time in this study. Our results are further supported by analyses of genetic distance, maximum likelihood and Bayesian inference, combined with different species delimitation approaches (distance-based vs. character-based).

The results from multiple markers, evaluated both separately and concatenated, consistently indicate that all Mediterranean specimens cluster in a unique group (Group 1, Clade A; Figs 2, 4–6). This batch of individuals is clearly separated by tens of mutations from the two other clusters composed only by the non-Mediterranean specimens (CE Atlantic and Indian Oceans) (Groups 2 and 3, Clades D and E; Figs 2, 4–6).

The occurrence of common shared haplotypes among western, central and eastern locations of the Mediterranean Sea suggests the lack of significant genetic differentiation among sites and corroborates the hypothesis of a lack of geographic segregation in the region. In Clade A, some haplotypes were shared across wider geographic ranges; for instance, the same haplotypes (e.g. COI_H1, ND2_H1, 16SH1 and 16SH2) occurred in not only the Mediterranean Sea, but also in the Atlantic, Indian and Pacific Oceans. Haplotype sharing among conspecifics can indicate that several allopatric populations are, in fact, part of a cosmopolitan species, characterized by significant gene-flow (Moura *et al.*, 2008). The genetic similarity could be explained by a reduction in the molecular evolution rate in this taxon, possibly due to long generation times associated with the extreme longevity of these organisms. Moreover, the existence of deep-water marine superhighways may facilitate long-distance movement and the connectivity across wide ranges (Moura *et al.*, 2008, 2015; Naylor *et al.*, 2012b; Veríssimo *et al.*, 2012; Bineesh *et al.*, 2017). However, the sharing of haplotypes among distant locations could be the consequence of limited resolution of the examined genes at the intraspecific level (Moura *et al.*, 2008).

Our current genetic results clearly support the hypothesis of a single species of *Centrophorus* inhabiting the Mediterranean waters. This was suggested by several authors in the past, but never objectively verified with a broader sampling (White *et al.*, 2013; Veríssimo *et al.*, 2014; Cariani *et al.*, 2017; Vella *et al.*, 2017 and references therein). Over the years, this Mediterranean taxon has been reported in papers and fishery statistics under different scientific names, creating confusion and raising the doubt that more than one species occurs in the basin. In their work, Guallart & Vicent (2001) proposed that the studied species be referred to as *Centrophorus granulosus* Bloch & Schneider, 1801 (*sensu* Müller & Henle, 1839), pending revision by the International Commission on Zoological Nomenclature (ICZN). Later, several authors argued that it was advisable to use a different name combination for individuals of Mediterranean

origin (for a detailed discussion see: White *et al.*, 2013, 2017; Verissimo *et al.*, 2014, Vella *et al.*, 2017). However, even in recent publications, the name *C. granulosus* (Cariani *et al.*, 2017; Ramírez-Amaro *et al.*, 2020) or *C.* cf. *granulosus* (Follesa *et al.*, 2019b; Leonetti *et al.*, 2020) was used to indicate the common Mediterranean gulper sharks, applying the precautionary principle. In some of our earlier publications (Cariani *et al.*, 2017, Follesa *et al.*, 2019b), we also reported the possible occurrence in the Mediterranean Sea of two different species, with the majority of individuals ascribed to *C. granulosus* and a few individuals reported under a different name (*C. uyato*), based merely on their original morphological identification in the field, which could not be tested (confirmed or disproved) by genetic tools. However, we are fully aware that identification by non-taxonomists, especially during fishery monitoring activities on-board, is susceptible to errors (Cariani *et al.*, 2017). For instance, in this study, the vast majority (about 87%) of Mediterranean specimens that clustered together in Clade A were a priori classified as *C. granulosus*, only a few as *C. uyato* (about 2%) and the remaining (about 11%) were only identified to the genus level as *Centrophorus* sp. (Supporting Information, Table S1).

It is beyond the scope of this paper to address the issue of the proper name to be used for *Centrophorus* individuals occurring in the Mediterranean Sea, or to retrace the long, controversial taxonomic diatribe related to them, since this has been well described in recent papers (Guallart, 1998; White *et al.*, 2013, 2017; Veríssimo *et al.*, 2014). However, a single, unambiguous species name for the Mediterranean gulper shark is fundamental to reduce the confusion about this taxon and to implement the correct attribution of specimens, with implications for the conservation and management of this genus. In light of this, we suggest conforming to the recommendation by White *et al.* (2013), which is now widely adopted by the scientific community, to use the name *C.* cf. *uyato* (or *C.* '*uyato*' *sensu* White *et al.*, 2013) for the gulper shark in the Mediterranean Sea, as well as for the conspecific specimens from the Atlantic, the Indian and the Pacific Oceans, and to use *C. granulosus* when referring to the largest member of this genus, which does not occur in Mediterranean waters (White *et al.*, 2013). Consequently, the specimens commonly found in the Mediterranean and attributed to *C. granulosus* (*C.* cf. *granulosus*) in previous papers (Cariani *et al.*, 2017; Follesa *et al.*, 2019b; Leonetti *et al.*, 2020; Ramírez-Amaro *et al.*, 2020) should be referred to as *C.* cf. *uyato* (*C.* '*uyato*' *sensu* White *et al.*, 2013). This new information on the genus confirms the importance of a revision of the identification field guides used in the Mediterranean, as suggested in Vella *et al.* (2017).

New genetic data for *Centrophorus* outside of the Mediterranean Sea

All the specimens from South Africa (Indian Ocean) were morphologically attributed, and then genetically assigned, to a single species: *C. squamosus*. Mauritania, in the central-eastern Atlantic Ocean, was the only location we analysed where specimens clustered in three different genetic clades, corresponding to Clades A, D and E, identified in the North Atlantic by Veríssimo *et al.* (2014). These results are in line with those presented for Portuguese waters, NE Atlantic, by Moura *et al.* (2015), where at least three species coexisted: *C. granulosus* (or the 'true' *C. granulosus sensu* White *et al.*, 2013), *C.* '*uyato*' (or *C.* cf. *uyato sensu* Veríssimo *et al.*, 2014) and *C. squamosus*. Once again, although *C. squamosus* was easily distinguished from other species based on its peculiar morphological features (i.e. dermal denticles) and hence correctly identified, in most cases, the initial morphological identification of the other CE Atlantic specimens did not correspond to their genetic clustering. Specimens visually identified as *C. granulosus* were genetically attributed to *C.* cf. *uyato* and specimens not identified at the species level were genetically ascribed to true *C. granulosus* (Supporting Information, Table S1).

We must consider that *C. squamosus* may occasionally enter the western part of the Mediterranean Basin from the Atlantic Ocean (Veríssimo *et al.*, 2014). This possibility is supported by the finding of a sequence from a Mediterranean specimen (collected in Algeria) reported by Veríssimo *et al.* (2014) clustering with other *C. squamosus* sequences. However, no photo voucher of this specimen is available and no morphological examination was possible (Veríssimo *et al.*, 2014). Other historical records of *C. squamosus* in the Mediterranean Sea exist, but they are not based on direct observations and hence were attributed to errors in taxon names or locality data of the specimens (Veríssimo *et al.*, 2014 and references therein). No confirmed occurrence of this species is available from any Mediterranean deep-water surveys carried out during the 20th century.

As already discussed for *C.* '*uyato*', *C. granulosus* and *C. squamosus* showed shared haplotypes among distant locations, ranging from Atlantic waters to the southern seas off Australia (Supporting Information, Tables S2–S5). This result highlights the high genetic similarity and the high gene-flow along the huge geographic distribution of the two species. Genetic homogeneity between eastern North Atlantic and South African populations of *C. squamosus* was detected and explained by the high dispersal in deep-water benthopelagic sharks, facilitated by the presence of continuous continental and insular slope habitats (Veríssimo *et al.*, 2012). The absence of genetic

divergence was found both at mitochondrial and nuclear loci (microsatellites), suggesting an ongoing or recent gene-flow among the locations investigated in the Atlantic, but not with a *C. squamosus* population from New Zealand (Veríssimo *et al.*, 2012).

Comparison with public data

Sequences for mitochondrial genes under investigation were available for 11 out of the 15 valid species of *Centrophorus* and for four out of the five species of *Deania*, as listed in Fricke *et al.* (2021). Unfortunately, sequence data for additional relevant taxa (e.g. *Centrophorus tesselatus* Garman, 1906 and *Centrophorus westraliensis* White *et al.*, 2008) and geographical areas from several previous molecular research works have not been deposited in GenBank or BOLD (Daley *et al.*, 2012; Naylor *et al.*, 2012a, b; Straube *et al.*, 2013; White *et al.*, 2013, 2017).

When sequenced data from online repositories were included in the alignments, evidence of identification problems was found in Centrophoridae, in both *Centrophorus* and *Deania*. It is a well-known problem that public repositories are especially prone to errors derived from misidentified specimens when collected and included into repositories with their original, incorrectly assigned, identities (Naylor *et al.*, 2012a). Incorrect names were found not only associated with sequences that were not included in publications (see Supporting Information, Tables S2–S4), but even for sequences that appeared in papers with different names from that used online (Douady *et al.*, 2003; Veríssimo *et al.*, 2014; Vella *et al.*, 2017). The confusion was also generated by sequences that were originally attributed to a species and later recognized as being part of a different taxon after a new species had been recognized or an existing species revised (e.g. *C. leslei* and *C. longipinnis*); their record in the public databases is never updated (Douady *et al.*, 2003; Wong *et al.*, 2009; Straube *et al.*, 2010; Costa *et al.*, 2012; Naylor *et al.*, 2012a, b; White *et al.*, 2017). It has been pointed out that once a name has been added to a database, it is difficult to convince data managers that it should be changed (Collins & Cruickshank, 2013).

The three markers evaluated in this study performed differently. For instance, the 16S gene allows discrimination of all *Centrophorus* species, except for *C. harrissoni/isodon* which share the same haplotype, as already pointed out by Daley *et al.* (2012). Moreover, the low variability of this fragment and the presence of singletons (unique haplotypes) compromised the ability of the BCMA to distinguish between *C. harrissoni*/*isodon* and *Centrophorus* sp. 1 or *C. squamosus* ($MOTU_1$) from *C. longipinnis* ($MOTU_2$).

COI proved to be more successful in distinguishing species. The trees (Fig. 4; Supporting Information, Figs S4, S5) and outputs of the BCMA analyses were able to recognize as separate MOTUs, sequences assigned by the BOLD RESL method to the same BIN. As expected, when singletons (unique haplotypes) are involved, the BCMA struggles to distinguish these MOTUs (Meier *et al.*, 2006; Brown & Collins, 2011).

A finer resolution was obtained with the fast-evolving protein-coding gene NADH dehydrogenase subunit 2 (*ND2*), which proved to be the most variable and informative in distinguishing among closely related species, even if they were represented by single haplotypes (e.g. *Centrophorus* sp. 1/*leslei*/*harrissoni*/*isodon* and *C. longipinnis*/cf. *longipinnis*, in Fig. 6 and Supporting Information, Figs S8, S9).

Considering that several species have been recently revised and other species and species-groups are at present under revision by expert taxonomists (Naylor *et al.*, 2012b; White *et al.*, 2013, 2017), we do not discuss in detail the several incongruencies that have emerged from the molecular data. Instead, we refer to two interesting points. First, the sharing of haplotypes among separate 'valid' species, for which several authors have proposed synonymizing two/three under the same name (e.g. *C.* cf. *uyato*/*Centrophorus zeehaani* White *et al.*, 2008, *C. granulosus*/*Centrophorus acus*, Garman, 1906/*C. niaukiang* Teng, 1959/*C. lusitanicus*; Naylor *et al.*, 2012a, b; White *et al.*, 2013, 2017; Veríssimo *et al.*, 2014; Moura *et al.*, 2015). As mentioned above, this could reflect incongruence between gene and species trees (different species that retain polymorphisms of the ancestral species from which they originated) or, more commonly, misidentification/mislabelling in the deposited sequences (Moura *et al.*, 2008). Second, our analyses indicate how undescribed species could exist within Centrophoridae (e.g. *C. cf. longipinnis* and *C.* cf. *isodon*) or that existing species should be split in two (e.g. the genetically distinct *C. atromarginatus* and *D. quadrispinosa* from the Indian and the Pacific Ocean). Confusion within this taxon is thus far from being resolved; additional studies should be carried out, based on a comprehensive sampling across the geographic range of all species, and analyses combining multiple molecular markers and morphological characters on verified individuals.

Molecular diagnostic characters to identify specimens

Because the genetic distance-based approach towards species identification lacks the specificity needed for regulatory or legal applications, which require unambiguous identification results, the identification of discrete molecular characters has been successfully applied to unambiguously diagnose species of elasmobranchs (Wong *et al.*, 2009; Vargheese *et al.*, 2019). Here, we have applied this approach, which has

allowed identification of tens of diagnostic species-specific nucleotide characters in the newly generated sequences. These characters can be easily used and strongly confirm the distinction of the three species under investigation: *C. granulosus*, *C. squamosus* and *C.* cf. *uyato* (Supporting Information, Table S6). The diagnostic nucleotide keys can be extremely useful to assign specimens to species, using a complementary methodology other than standard sequencing; for instance, to design species-specific probes for microarrays or to identify species-specific primers to use in multiplex PCR assays.

Our results show how the number of diagnostic characters decreased as the whole pool of specimen haplotypes and species increased, including all sequence data available for the family Centrophoridae (Supporting Information, Table S7). This is not surprising, because diagnostic nucleotides are less likely to be present as the variability in character states reaches saturation (Wong *et al.*, 2009). In particular, it has been proven that the addition of a closely related species in the pool of sequences is more likely to eliminate a previously identified diagnostic nucleotide (Wong *et al.*, 2009). However, to address our specific problem, namely the correct identification of Mediterranean *Centrophorus* specimens, we should focus on key diagnostic characters obtained by comparing the sequences of the three candidate species in our area of interest. It is unnecessary to include in the analyses sequences of species that do not occur in the area, since when enlarging the pool of sequences/species it would only reduce the number of diagnostic characters without any beneficial effect.

Morphometric assessment

The CAP analysis strongly confirms the a priori genetic group assignments, identifying three distinct groups with different morphotypes. Interestingly, the morphometric measures that have been recognized by the SIMPER analysis as being responsible for the majority of intraspecific similarity are all related to the head and trunk, suggesting a greater influence of the main body shape in group identification, rather than the fin morphology. In particular, *C. granulosus* shows, on average, shorter head and trunk measurements related to the total length (TL) than the other two groups. However, given the small sample size of specimens belonging to this species, these results should be considered as preliminary and provided as mostly useful for species descriptive/qualitative analyses. These results are in agreement with White *et al.* (2013) and Veríssimo *et al.* (2014), with the exception of the prebranchial length (PG1) and interdorsal space (IDS). The former appeared smaller in the present study than those previously reported, while the latter was found to be higher than that reported in White *et al.* (2013), but in accordance with the study by Veríssimo *et al.* (2014). However, this difference could also reflect the fact that the IDS measurement in our study and Verissimo's refers to the 'distance from first dorsal fin insertion to second dorsal fin insertion', rather than to the 'distance from first dorsal fin insertion to second dorsal fin origin' as in White's study.

The most important measure to discriminate the species appears to be the pectoral fin posterior lobe length (P1I), which clearly separates *C. squamosus* from the others. This result agrees with the literature, which often reports a short, not particularly sharp and not elongated pectoral free edge for this species (e.g. Ebert *et al.*, 2013), lying in the range reported by Veríssimo *et al.* (2014). Nevertheless, this structure is frequently ruined due to its fragile nature and it could also be easily damaged because of particular mating behaviours, such as pectoral grasps or bites, reported in several shark species (e.g. White *et al.*, 2013; Afonso *et al.*, 2016; McCauley *et al.*, 2010). In addition, P1I represents a markedly allometric parameter, depending on the size of the specimens, as reported in Guallart (1998) and Guallart *et al.* (2013). For these reasons, the fin lobe should be carefully evaluated before being used for any identification attempt. In addition, most of the measurements recorded in this study for *C. squamosus* agree with those reported by Veríssimo *et al.* (2014), with the exception of the preventral caudal fin margin (CPV), the first dorsal fin height (D1H), the second dorsal fin anterior margin (D2A) and the second dorsal fin inner margin (D2I), which all measured less in the present study. This could be attributed to allometric factors, considering the wider TL range of the individuals analysed in this paper.

All Mediterranean specimens are correctly assigned to the *C.* cf. *uyato* group by the CAP analysis. This finding could be considered endorsed by the results of the secondary CAP analysis, which included the samples without molecular identification that grouped all Mediterranean specimens together.

Three individuals of *C.* cf. *uyato* caught in the Atlantic Ocean were in the external margin of their group clouds in the CAP analysis, pointing towards the other Atlantic shark groups (Fig. 7). This suggests that the Atlantic population may present some morphological features differentiating it from the Mediterranean one. These morphological dissimilarities could be due to a certain degree of isolation caused by the Strait of Gibraltar, not only because of its small amplitude, but also because of its shallow maximum depth (Fredj & Laubier, 1985) and/or to the adaptation to different environmental conditions, as observed also for other deep-sea sharks, such as *Centroscymnus coelolepis* Barbosa du Bocage & Brito Capello, 1864 (Catarino

et al., 2015). It is, indeed, widely reported that populations of the same species may exhibit various growth patterns related to the inhabited geographic area (Carlson *et al.*, 2003; Driggers *et al.*, 2004). This last hypothesis should be investigated further.

Even though the contribution of the linear measurements of fins in species discrimination is not the most relevant (as highlighted by the SIMPER analysis), the results of the geometric morphometry analyses (PCA, CVA, Procrustes ANOVA, pair-wise comparisons and DFA) consistently showed differences in the shape of the two dorsal fins and the caudal fins among species, more clearly in the comparison between *C.* cf. *uyato* and *C. squamosus*. Because of the small sample size, the results relative to *C. granulosus* should be taken with caution and considered preliminary. Future studies, based on larger sample sizes, will probably corroborate the evidence reported here. The samples of this species considered in the multivariate analyses on D1, D2 and C, were widely included within the samples of *C.* cf. *uyato*. Such differences in the shape of dorsal and caudal fins may be useful in the context of species identification, as these fins are usually less damaged by fishing operation than is body shape. The observed differences in fin morphology could reflect the occupation of habitats with different environmental characteristics (Sternes & Shimada, 2020). Even if the relationship between the morphometric variability and the ecological characteristics of species is still little explored, the high variability in the caudal fin shape may reflect the species-specific patterns of movement, feeding and habitat utilization (Thomson, 1976; Thomson & Simanek, 1977; Lauder, 2000; Wilga & Lauder, 2002; Scacco *et al.*, 2010; Kim *et al.*, 2013; Irschick & Hammerschlag, 2015; Irschick *et al.*, 2017; Sternes & Shimada, 2020).

In the specific case of *Centrophorus* species, the caudal fin displays a prominent asymmetry that is reported to be correlated with their general slow-swimming behaviour and their feeding habit, which may include predation on faster prey (Thomson, 1976; Thomson & Simanek, 1977; Scacco *et al.*, 2010; Irschick *et al.*, 2017). The caudal fin morphology could also be associated with their escape behaviour (Domenici *et al.*, 2004) and could represent an adaptation to the higher density of the deep-water masses they inhabit (Scacco *et al.*, 2010). However, limited information is currently available on the genus *Centrophorus* regarding biological, ecological and life-history traits. Further investigations are needed to improve our knowledge and to confirm our hypotheses.

Significative differences in the shape of the first and second dorsal fins were also detected. According to the literature, the role of the dorsal fins on the swimming ability and hydrodynamics of Centrophoridae is not well understood, but it is hypothesized to be related to the undulation shape that allows the animals to maintain their stability and manoeuvrability during swimming (Lingham-Soliar, 2005; Maia & Wilga, 2013a, b, 2016; Maia *et al.*, 2017).

Many structures, including the fins analysed in this work, have been demonstrated to be correlated with changes in feeding behaviour and the transition to different habitats during the lifespan of an individual (Fu *et al.*, 2016; Bernal-Durán & Landaeta, 2017; Ventura *et al.*, 2017; Martinez *et al.*, 2018; Wilson *et al.*, 2020). Because ontogenetic morphological variation has been reported in *C.* cf. *uyato* (Guallart, 1998; Guallart *et al.*, 2013; White *et al.*, 2013, 2017; Veríssimo *et al.*, 2014), we also performed some intraspecific analyses to investigate the structural variations of this species over its lifespan. According to our results, no significant difference was found between male and female specimens, so the presence of sexual dimorphism in the fin shape was excluded. The two regression models performed suggest the presence of significant ontogenetic shape change. However, this interpretation must be taken with caution because, in particular for dorsal fins, specimens with a total length less than 70 cm and more than 100 cm are severely under-represented in the dataset. If these tendencies were confirmed, we could hypothesize that the change in ontogenetic shape may reflect the ability of different life-stages of this species to occupy different habitats, changing their ecology and feeding behaviour over time (Fu *et al.*, 2016; Irschick *et al.*, 2017). This evidence could be supported by previous studies conducted on *Centrophorus* species, which reported bathymetric segregation by sex, size and maturity (Golani & Pisanty, 2000; Clarke *et al.*, 2001; Megalofonou & Chatzispyrou, 2006; Bañón *et al.*, 2008; Rodríguez-Cabello & Sánchez, 2014; Cotton *et al.*, 2015; Rodríguez-Cabello *et al.*, 2016; Lteif *et al.*, 2017). The few studies performed on the species of *Centrophorus* inhabiting the Mediterranean Basin, reported here as *C.* cf. *uyato*, have confirmed that this species occupies different depth-layers according to its size (Golani & Pisanty, 2000; Megalofonou & Chatzispyrou, 2006).

Differences in dorsal fin shape are used broadly to distinguish and identify specimens at different taxonomic levels (Andreotti *et al.*, 2018; Yahn *et al.*, 2019) confirming the reliability of this approach for the purposes of our study. In this perspective, the creation of a public database of shark fins, along with the implementation of the landmarks-based techniques, could promote the development of reliable and easy-to-use tools for a quick identification in the field (http://www.fao.org/ipoa-sharks/tools/software/isharkfin/en/).

In conclusion, the current study provides important information on the presence of a unique, undescribed species of *Centrophorus* in the Mediterranean Sea, which we tentatively identify as *C.* cf. *uyato*, as previously proposed by Veríssimo *et al.* (2014).

Therefore, a single unambiguous and taxonomically valid name for the Mediterranean gulper shark should be described following the proper procedure of the ICZN, along with the designation of a holotype to reduce the confusion bearing upon this species. Looking forward to a comprehensive taxonomic revision of the genus *Centrophorus*, the implementation of the correct assignment of the specimens will improve the management and conservation of these species.

ACKNOWLEDGEMENTS

We thank Maria Teresa Spedicato for her contribution in implementing the research network among the institutes involved in the Mediterranean International Trawl Survey (MEDITS) and Simone Di Crescenzo for his help with sampling. We also thank all participants of the MEDITS surveys and the crews of each research vessel. The editors are thanked for valuable comments that improved the manuscript.

This research was partially funded by the University of Bologna through 'RFO' and 'Canziani' grants given to FT and AC and by the European Commission Directorate – General Fisheries in the framework of the MEDITS survey. RM and LC acknowledge the support for their research grants to funds granted by the Università degli Studi di Cagliari 'UNICA-RICCAR_2013_CAU_02' and Ministero dell'Università e della Ricerca 'PON AIM 1854833 - PON Ricerca e Innovazione 2014-2020 – Azione I.2 - D.D. n. 407, 27/02/2018 – Attraction and International Mobility', respectively. The funders had no role in study design, data collection and analysis, decision to publish or preparation of the manuscript. The authors declare that they have no relevant financial or non-financial conflict of interests in the subject matter or materials discussed in this manuscript.

DATA AVAILABILITY

Sequences and data on specimens are available on GenBank and Bold databases, as specified in the main text.

REFERENCES

Afonso AS, **Cantareli CV**, **Levy RP**, **Veras lB. 2016.** Evasive mating behaviour by female nurse sharks, *Ginglymostoma cirratum* (Bonnaterre, 1788), in an equatorial insular breeding ground. *Neotropical Ichthyology* **14:** e160103.

Andreotti S, **Holtzhausen P**, **Rutzen M**, **Meÿer M**, **Van der Walt S**, **Herbst B**, **Matthee CA. 2018.** Semi-automated software for dorsal fin photographic identification of marine species: application to *Carcharodon carcharias*. *Marine Biodiversity* **48:** 1655–1660.

Bañón R, **Piñeiro C**, **Casas M. 2008.** Biological observations on the gulper shark *Centrophorus granulosus* (Chondrichthyes: Centrophoridae) off the coast of Galicia (north-western Spain, eastern Atlantic). *Journal of the Marine Biological Association of the UK* **88:** 411–414.

Bellodi A, **Porcu C**, **Cau A**, **Marongiu MF**, **Melis R**, **Mulas A**, **Pesci P**, **Follesa MC**, **Cannas R. 2018.** Investigation on the genus *Squalus* in the Sardinian waters (central-western Mediterranean) with implications on its management. *Mediterranean Marine Science* **19:** 256–272.

Bernal-Durán V, **Landaeta MF. 2017.** Feeding variations and shape changes of a temperate reef clingfish during its early ontogeny. *Scientia Marina* **81:** 205–215.

Bineesh KK, **Gopalakrishnan A**, **Akhilesh KV**, **Sajeela KA**, **Abdussamad EM**, **Pillai NGK**, **Basheer VS**, **Jena JK**, **Ward RD. 2017.** DNA barcoding reveals species composition of sharks and rays in the Indian commercial fishery. *Mitochondrial DNA A DNA Mapp Seq Anal* **28:** 458–472.

Boroni NL, **Lobo LS**, **Romano PSR**, **Lessa G. 2017.** Taxonomic identification using geometric morphometric approach and limited data: an example using the upper molars of two sympatric species of *Calomys* (Cricetidae: Rodentia). *Zoologia* **34:** 1–11.

Brown SDJ, **Collins RA. 2011.** *Spider: species identity and evolution in R. A tutorial*. http://spider.r-forge.r-project.org/ (accessed 02 December 2021).

Brown SDJ, **Collins RA**, **Boyer S**, **Lefort M-C**, **Malumbres-Olarte J**, **Vink CJ**, **Cruickshank RH. 2012.** Spider: an R package for the analysis of species identity and evolution, with particular reference to DNA barcoding. *Molecular Ecology Resources* **12:** 562–565.

Cadenat J, **Blache J. 1981.** *Requins de Méditerranée et d'Atlantique (plus particulièrement de la Côte occidentale d'Afrique) – collection faune tropicale, no. XXI*. Paris: Editions de l'Office de la Recherche scientifique et Technique Outre-Mer.

Cariani A, **Messinetti S**, **Ferrari A**, **Arculeo M**, **Bonello JJ**, **Bonnici L**, **Cannas R**, **Carbonara P**, **Cau A**, **Charilaou C**, **El Ouamari N**, **Fiorentino F**, **Follesa MC**, **Garofalo G**, **Golani D**, **Guarniero I**, **Hanner R**, **Hemida F**, **Kada O**, **Lo Brutto S**, **Mancusi C**, **Morey G**, **Schembri PJ**, **Serena F**, **Sion L**, **Stagioni M**, **Tursi A**, **Vrgoc N**, **Steinke D**, **Tinti F. 2017.** Improving the conservation of Mediterranean Chondrichthyans: the ELASMOMED DNA barcode reference library. *PLoS One* **12:** e0170244.

Carlson JK, **Cortés E**, **Bethea D. 2003.** Life history and population dynamics of the finetooth shark, *Carcharhinus isodon,* in the northeastern Gulf of Mexico. *Fishery Bulletin* **101:** 281–292.

Cartes JE, **Maynou F**, **Sardà F**, **Company JB**, **Lloris D**, **Tudela S. 2004.** The Mediterranean deep-sea ecosystems: an overview of their diversity, structure, functioning and anthropogenic impacts. Part I. In: *The Mediterranean deep-sea ecosystems: an overview of their diversity, structure, functioning and anthropogenic impacts, with a proposal for conservation*. IUCN Málaga and WWF Rome, 9–38.

Catarino D, **Knutsen H**, **Veríssimo A**, **Olsen EM**, **Jorde PE**, **Menezes G**, **Sannæs H**, **Stanković D**, **Company JB**, **Neat F**, **Danovaro R. 2015.** The Pillars of Hercules as a bathymetric barrier to gene flow promoting isolation in a global deep-sea shark (*Centroscymnus coelolepis*). *Molecular Ecology* **24:** 6061–6079.

Chuang P-S, **Hung T-C**, **Chang H-A**, **Huang C-K**, **Shiao J-C. 2016.** The species and origin of shark fins in Taiwan's fishing ports, markets, and customs detention: a DNA barcoding analysis. *PLoS One* **11:** e0147290.

Clarke KR, **Gorley RN. 2015.** *PRIMER v.7: user manual / tutorial*. Plymouth: PRIMER-E. Available at: http://www.primer-e.com/. (accessed 14 November 2021).

Clarke MW, **Connolly PL**, **Bracken JJ. 2001.** Aspects of reproduction of the deep water sharks *Centroscymnus coelolepis* and *Centrophorus squamosus* from west of Ireland and Scotland. *Journal of the Marine Biological Association of the UK* **81:** 1019–1029.

Coll M, **Piroddi C**, **Steenbeek J**, **Kaschner K**, **Lasram FBR**, **Aguzzi J**, **Ballesteros E**, **Bianchi CN**, **Corbera J**, **Dailianis T**, **Danovaro R**, **Estrada M**, **Froglia C**, **Galil BS**, **Gasol JM**, **Gertwagen R**, **Gil J**, **Guilhaumon F**, **Kesner-Reyes K**, **Kitsos M-S**, **Koukouras A**, **Lampadariou N**, **Laxamana E**, **Lopez-Fe de la Cuadra CM**, **Lotze HK**, **Martin D**, **Mouillot D**, **Oro D**, **Raicevich S**, **Rius-Barile J**, **Ignacio Saiz-Salinas J**, **San Vicente C**, **Somot S**, **Templado J**, **Turon X**, **Vafidis D**, **Villanueva R**, **Voultsiadou E. 2010.** The biodiversity of the Mediterranean Sea: estimates, patterns, and threats. *PLoS One* **5:** e11842.

Collins RA, **Cruickshank RH. 2013.** The seven deadly sins of DNA barcoding. *Molecular Ecology Resources* **13:** 969–975.

Compagno LJV. 1984. *FAO species catalogue. Vol. 4. Sharks of the world. An annotated and illustrated catalogue of shark species known to date. Part 1. Hexanchiformes to Lamniformes*. Rome: FAO.

Compagno LJV. 2001. *Sharks of the world. An annotated and illustrated catalogue of shark species known to date. Vol. 2. Bullhead, mackerel and carpet sharks (Heterodontiformes, Lamniformes and Orectolobiformes)*. **Report No. 1, Vol. 2**. Rome: FAO.

Costa FO, **Landi M**, **Martins R**, **Costa MH**, **Costa ME**, **Carneiro M**, **Alves MJ**, **Steinke D**, **Carvalho GR. 2012.** A ranking system for reference libraries of DNA barcodes: application to marine fish species from Portugal. *PLoS One* **7:** e35858.

Cotton CF, **Dean Grubbs R**, **Dyb JE**, **Fossen I**, **Musick JA. 2015.** Reproduction and embryonic development in two species of squaliform sharks, *Centrophorus granulosus* and *Etmopterus princeps*: evidence of matrotrophy? *Deep Sea Research Part II: Topical Studies in Oceanography, Biology of Deep-Water Chondrichthyans* **115:** 41–54.

Daley RK, **Appleyard SA**, **Koopman M. 2012.** Genetic catch verification to support recovery plans for deepsea gulper sharks (genus *Centrophorus*, family Centrophoridae) – an Australian example using the 16S gene. *Marine and Freshwater Research* **63:** 708–714.

Darriba D, **Taboada G**, **Doallo R**, **Posada D. 2012.** jModelTest 2: more models, new heuristics and parallel computing. *Nature Methods* **9:** 772.

Dayrat B. 2005. Toward integrative taxonomy. *Biological Journal of the Linnean Society* **85:** 407–415.

Domenici P, **Standen E**, **Levine R. 2004.** Escape manoeuvres in the spiny dogfish (*Squalus acanthias*). *Journal of Experimental Biology* **207:** 2339–2349.

Douady CJ, **Dosay M**, **Shivji MS**, **Stanhope MJ. 2003.** Molecular phylogenetic evidence refuting the hypothesis of Batoidea (rays and skates) as derived sharks. *Molecular Phylogenetics and Evolution* **26:** 215–221.

Driggers WB III, **Carlson JK**, **Oakley D**, **Ulrich G**, **Cullum B**, **Dean JM. 2004.** Age and growth of the blacknose shark, *Carcharhinus acronotus*, in the western North Atlantic Ocean with comments on regional variation in growth rates. *Environmental Biology of Fishes* **71:** 171–178.

Dulvy NK, **Baum JK**, **Clarke S**, **Compagno LJV**, **Cortes E**, **Domingo A**, **Fordham S**, **Fowler S**, **Francis MP**, **Gibson C**, **Martinez J**, **Musick JA**, **Soldo A**, **Stevens JD**, **Valenti S. 2008.** You can swim but you can't hide: the global status and conservation of oceanic pelagic sharks and rays. *Aquatic Conservation: Marine and Freshwater Ecosystems* **18:** 459–482.

Ebert DA, **Fowler S**, **Compagno LJV. 2013.** *Sharks of the world. A fully illustrated guide*. Plymouth: Wild Nature Press, 528.

Excoffier L, **Lischer H. 2010.** ARLEQUIN suite v. 3.5: a new series of programs to perform population genetics analyses under Linux and Windows. *Molecular Ecology Resources* **10:** 564–567.

Felsenstein J. 1985. Confidence limits on phylogenies: an approach using the bootstrap. *Evolution* **39:** 783–791.

Fernando D, **Bown RMK**, **Tanna A**, **Gobiraj R**, **Ralicki H**, **Jockusch EL**, **Ebert DA**, **Jensen K**, **Caira JN. 2019.** New insights into the identities of the elasmobranch fauna of Sri Lanka. *Zootaxa* **4585:** 201–238.

Ferretti F, **Worm B**, **Britten GL**, **Heithaus MR**, **Lotze HK. 2010.** Patterns and ecosystem consequences of shark declines in the ocean. *Ecology Letters* **13:** 1055–1071.

Follesa MC, **Agus B**, **Bellodi A**, **Cannas R**, **Capezzuto F**, **Casciaro L**, **Cau A**, **Cuccu D**, **Donnaloia M**, **Fernandez-Arcaya U**, **Gancitano V**, **Gaudio P**, **Marongiu MF**, **Mulas A**, **Pesci P**, **Porcu C**, **Rossetti I**, **Sion L**, **Vallisneri M**, **Carbonara P. 2019a.** The MEDITS maturity scales as a useful tool for investigating the reproductive traits of key species in the Mediterranean Sea. *Scientia Marina* **83S1:** 235–256.

Follesa MC, **Marongiu MF**, **Zupa W**, **Bellodi A**, **Cau A**, **Cannas R**, **Colloca F**, **Djurovic M**, **Isajlovic I**, **Jadaud A**, **Manfredi C**, **Mulas A**, **Peristeraki P**, **Porcu C**, **Ramirez-Amaro S**, **Salmerón Jiménez F**, **Serena F**, **Sion L**, **Thasitis I**, **Cau A**, **Carbonara P. 2019b.** Spatial variability of Chondrichthyes in the northern Mediterranean. *Scientia Marina* **83:** 81.

Fredj G, **Laubier L. 1985.** *The deep Mediterranean benthos*. In: Moraitou-Apostolopoulu M, Kiortsis V, eds. *Mediterranean marine ecosystems*. New York: Plenum Press, 109–145.

Frodella N, **Cannas R**, **Velona A**, **Carbonara P**, **Farrell ED**, **Fiorentino F**, **Follesa MC**, **Garofalo G**, **Hemida F**, **Mancusi C**, **Stagioni M**, **Ungaro N**, **Serena F**,

Tinti F, **Cariani A. 2016.** Population connectivity and phylogeography of the Mediterranean endemic skate *Raja polystigma* and evidence of its hybridization with the parapatric sibling *R. montagui*. *Marine Ecology Progress Series* **554:** 99–113.

Fricke R, Eschmeyer WN, Van der Laan R, eds. 2021. *Eschmeyer's catalog of fishes: genera, species, references*. Available at: http://researcharchive.calacademy.org/research/ichthyology/catalog/fishcatmain.asp (accessed 14 November 2021).

Fu AL, **Hammerschlag N**, **Lauder GV**, **Wilga CD**, **Kuo C-Y**, **Irschick DJ. 2016.** Ontogeny of head and caudal fin shape of an apex marine predator: the tiger shark (*Galeocerdo cuvier*). *Journal of Morphology* **277:** 556–564.

Gadagkar S, **Rosenberg M**, **Kumar S. 2005.** Inferring species phylogenies from multiple genes: concatenated sequence tree versus consensus gene tree. *Journal of Experimental Zoology Part B Molecular and Developmental Evolution* **304:** 64–74.

García VB, **Lucifora LO**, **Myers RA. 2008.** The importance of habitat and life history to extinction risk in sharks, skates, rays and chimaeras. *Proceedings of the Royal Society B: Biological Sciences* **275:** 83–89.

Golani D, **Pisanty S. 2000.** Biological aspects of the Gulper shark, *Centrophorus granulosus* (Bloch and Schneider, 1801), from the Mediterranean coast of Israel. *Acta Adriatica* **41:** 71–77.

Guallart J. 1998. *Contribuciòn al conocimientto de la taxonomüa y la biologüa del tiburón batial* Centrophorus granulosus *(Bloch & Schneider, 1801) (Elasmobranchii, Squalidae) en el Mar Balear (Mediterráneo occidental)*. Unpublished D. Phil. Thesis, University of Valencia.

Guallart J, **Vicent JJ. 2001.** Changes in composition during embryo development of the gulper shark, *Centrophorus granulosus* (Elasmobranchii, Centrophoridae): an assessment of maternal-embryonic nutritional relationships. *Environmental Biology of Fishes* **61:** 135–150.

Guallart J, **García-Salinas P**, **Catalán A. 2013.** Morphometric ontogenetic changes in the little gulper shark *Centrophorus granulosus* (Squaliformes, Centrophoridae) from the Mediterranean Sea: a critical review of anatomic characters used for species discrimination within the genus. In: European Elasmobranch Association, *Book of Abstracts, 17th European Elasmobranch Association Conference 2013*. Plymoth: Plymouth University, 74.

Guillaud E, **Cornette R**, **Béarez P. 2016.** Is vertebral form a valid species-specific indicator for salmonids? The discrimination rate of trout and Atlantic salmon from archaeological to modern times. *Journal of Archaeological Science* **65:** 84–92.

Guindon S, **Gascuel O. 2003.** A simple, fast, and accurate algorithm to estimate large phylogenies by maximum likelihood. *Systematic Biology* **52:** 696–704.

Guindon S, **Dufayard J-F**, **Lefort V**, **Anisimova M**, **Hordijk W**, **Gascuel O. 2010.** New algorithms and methods to estimate maximum-likelihood phylogenies: assessing the performance of PhyML 3.0. *Systematic Biology* **59:** 307–321.

Hasegawa M, **Kishino H**, **Yano T. 1985.** Dating of the human-ape splitting by a molecular clock of mitochondrial DNA. *Journal of Molecular Evolution* **22:** 160–174.

Henderson AC, **Reeve AJ**, **Jabado RW**, **Naylor GJP. 2016.** Taxonomic assessment of sharks, rays and guitarfishes (Chondrichthyes: Elasmobranchii) from south-eastern Arabia, using the NADH dehydrogenase subunit 2 (NADH2) gene. *Zoological Journal of the Linnean Society* **176:** 399–442.

Ibáñez AL, **Jawad LA. 2018.** Morphometric variation of fish scales among some species of rattail fish from New Zealand waters. *Journal of the Marine Biological Association of the UK* **98:** 1991–1998.

Irschick DJ, **Hammerschlag N. 2015.** Morphological scaling of body form in four shark species differing in ecology and life history. *Biological Journal of the Linnean Society* **114:** 126–135.

Irschick DJ, **Fu A**, **Lauder G**, **Wilga C**, **Kuo C-Y**, **Hammerschlag N. 2017.** A comparative morphological analysis of body and fin shape for eight shark species. *Biological Journal of the Linnean Society* **122:** 589–604.

Kim SH, **Shimada K**, **Rigsby CK. 2013.** Anatomy and evolution of heterocercal tail in lamniform sharks. *The Anatomical Record* **296:** 433–442.

Kimura M. 1980. A simple method for estimating evolutionary rates of base substitutions through comparative studies of nucleotide sequences. *Journal of Molecular Evolution* **16:** 111–120.

Klingenberg C. 2011. MorphoJ: an integrated software package for geometric morphometrics. *Molecular Ecology Resources* **11:** 353–357.

Kumar S, **Stecher G**, **Tamura K. 2016.** MEGA7: molecular evolutionary genetics analysis version 7.0 for bigger datasets. *Molecular Biology and Evolution* **33:** 1870–1874.

Lauder GV. 2000. Function of the caudal fin during locomotion in fishes: kinematics, flow visualization, and evolutionary patterns. *Integrative and Comparative Biology* **40:** 101–122.

Leonetti F, **Giglio G**, **Leone A**, **Coppola F**, **Romano C**, **Bottaro M**, **Reinero F**, **Milazzo C**, **Micarelli P**, **Tripepi S**, **Sperone E. 2020.** An updated checklist of chondrichthyans of Calabria (Central Mediterranean, southern Italy), with emphasis on rare species. *Mediterranean Marine Science* **21:** 794–807.

Lingham-Soliar T. 2005. Dorsal fin in the white shark, *Carcharodon carcharias*: a dynamic stabilizer for fast swimming. *Journal of Morphology* **263:** 1–11.

Lteif M, **Mouawad R**, **Khalaf G**, **Lenfant P**, **Seret B**, **Verdoit-Jarraya M. 2017.** Population biology of the little gulper shark *Centrophorus uyato* in Lebanese waters. *Journal of Fish Biology* **91:** 1491–1509.

Maia A, **Wilga CA. 2013a.** Function of dorsal fins in bamboo shark during steady swimming. *Zoology* **116:** 224–231.

Maia A, **Wilga CA. 2013b.** Anatomy and muscle activity of the dorsal fins in bamboo sharks and spiny dogfish during turning maneuvers. *Journal of Morphology* **274:** 1288–1298.

Maia A, **Wilga CA. 2016.** Dorsal fin function in spiny dogfish during steady swimming. *Journal of Zoology* **298:** 139–149.

Maia A, **Lauder GV**, **Wilga CD. 2017.** Hydrodynamic function of dorsal fins in spiny dogfish and bamboo sharks

during steady swimming. *Journal of Experimental Biology* **220:** 3967–3975.

Martinez CM, **McGee MD**, **Borstein SR**, **Wainwright PC. 2018.** Feeding ecology underlies the evolution of cichlid jaw mobility. *Evolution* **72:** 1645–1655.

McCauley DJ, **Papastamatiou YP**, **Young HS. 2010.** An observation of mating in free-ranging blacktip reef sharks, *Carcharhinus melanopterus*. *Pacific Science* **64:** 349–352.

Megalofonou P, **Chatzispyrou A. 2006.** Sexual maturity and feeding of the gulper shark, *Centrophorus granulosus*, from the eastern Mediterranean Sea. *Cybium* **30:** 67–74.

Meier R, **Shiyang K**, **Vaidya G**, **Ng PKL. 2006.** DNA barcoding and taxonomy in Diptera: a tale of high intraspecific variability and low identification success. *Systematic Biology* **55:** 715–728.

Meyer CP, **Paulay G. 2005.** DNA barcoding: error rates based on comprehensive sampling. *PLoS Biology* **3:** e422.

Morato T, **Watson R**, **Pitcher TJ**, **Pauly D. 2006.** Fishing down the deep. *Fish and Fisheries* **7:** 24–34.

Moura T, **Silva MC**, **Figueiredo I**, **Neves A**, **Muñoz PD**, **Coelho MM**, **Gordo LS. 2008.** Molecular barcoding of north-east Atlantic deep-water sharks: species identification and application to fisheries management and conservation. *Marine and Freshwater Research* **59:** 214–223.

Moura T, **Silva MC**, **Figueiredo I. 2015.** Barcoding deep-water chondrichthyans from mainland Portugal. *Marine and Freshwater Research* **66:** 508–517.

Muñoz-Chapuli R, **Ramos F. 1989.** Review of the *Centrophorus* sharks (Elasmobranchii, Squalidae) of the eastern Atlantic. *Cybium* **13:** 65–81.

Myers RA, **Worm B. 2003.** Rapid worldwide depletion of predatory fish communities. *Nature* **423:** 280–283.

Naylor G, **Caira J**, **Jensen K**, **Rosana K**, **Straube N**, **Lakner C. 2012a.** Elasmobranch phylogeny: a mitochondrial estimate based on 595 species. In: Carrier JC, Musick JA, Heithaus MR, eds. *Biology of sharks and their relatives*, *2nd edn*. Boca Raton: CRC Press, 31–56.

Naylor G, **Caira JN**, **Jensen K**, **Rosana KAM**, **White W**, **Last P. 2012b.** A DNA sequence–based approach to the identification of shark and ray species and its implications for global elasmobranch diversity and parasitology. *Bulletin of the American Museum of Natural History* **367:** 1–262.

Oliver S, **Braccini M**, **Newman SJ**, **Harvey ES. 2015.** Global patterns in the bycatch of sharks and rays. *Marine Policy* **54:** 86–97.

Ovenden J, **Berry O**, **Welch D**, **Buckworth R**, **Dichmont C. 2013.** Ocean's eleven: a critical evaluation of the role of population, evolutionary and molecular genetics in the management of wild fisheries. *Fish and Fisheries* **16:** 125–159.

Pinello D, **Gee J**, **Accadia P**, **Sabatella EC**, **Vitale S**, **Polymeros K**, **Fiorentino F. 2018.** Efficiency of shallow- and deep-water trawling in the Mediterranean and its implications for discard reduction. *Scientia Marina* **82S1:** 97–106.

Porcu C, **Bellodi A**, **Cau A**, **Cannas R**, **Marongiu MF**, **Mulas A**, **Follesa MC. 2020.** Uncommon biological patterns of a little known endemic Mediterranean skate, *Raja polystigma* (Risso, 1810). *Regional Studies in Marine Science* **34:** 101065.

Rach J, **DeSalle R**, **Sarkar IN**, **Schierwater B**, **Hadrys H. 2008.** Character-based DNA barcoding allows discrimination of genera, species and populations in Odonata. *Proceedings of the Royal Society B* **275:** 237–247.

Ramírez-Amaro S, **Ordines F**, **Picornell A**, **Castro JA**, **Ramon MM**, **Massutí E**, **Terrasa B. 2018.** The evolutionary history of Mediterranean Batoidea (Chondrichthyes: Neoselachii): a molecular phylogenetic approach. *Zoologica Scripta* **47:** 686–698.

Ramírez-Amaro S, **Ordines F**, **Esteban A**, **García C**, **Guijarro B**, **Salmerón F**, **Terrasa P**, **Massutí E. 2020.** The diversity of recent trends for chondrichthyans in the Mediterranean reflects fishing exploitation and a potential evolutionary pressure towards early maturation. *Scientific Reports* **10:** 547.

Ratnasingham S, **Hebert PDN. 2007.** BOLD: the barcode of life data system (www.barcodinglife.org). *Molecular Ecology Notes* **7:** 355–364.

Ratnasingham S, **Hebert PDN. 2013.** A DNA-based registry for all animal species: the Barcode Index Number (BIN) system. *PLoS One* **8:** e66213.

Rodríguez-Cabello C, **Sánchez F. 2014.** Is *Centrophorus squamosus* a highly migratory deep-water shark? *Deep Sea Research Part I: Oceanographic Research Papers* **92:** 1–10.

Rodríguez-Cabello C, **González-Pola C**, **Sánchez F. 2016.** Migration and diving behavior of *Centrophorus squamosus* in the NE Atlantic. Combining electronic tagging and Argo hydrography to infer deep ocean trajectories. *Deep Sea Research Part I: Oceanographic Research Papers* **115:** 48–62.

Rodríguez-Cabello C, **Pérez M**, **Grasa I. 2020.** Taxonomic research on *Deania calcea* and *Deania profundorum* (family: Centrophoridae) in the Cantabrian Sea (northeast Atlantic) with comments on *Deania hystricosa*. *Regional Studies in Marine Science* **37:** 101321.

Rohlf FJ. 1999. Shape statistics: procrustes superimpositions and tangent spaces. *Journal of Classification* **16:** 197–223.

Rohlf FJ. 2015. The Tps series of software. *Hystrix* **26:** 1–4.

Ronquist F, **Teslenko M**, **Mark P**, **Ayres D**, **Darling A**, **Höhna S**, **Larget B**, **Liu L**, **Suchard M**, **Huelsenbeck J. 2012.** MrBayes 3.2: efficient Bayesian phylogenetic inference and model choice across a large model space. *Systematic Biology* **61:** 539–542.

Rozas J, **Ferrer-Mata A**, **Sánchez-DelBarrio J**, **Guirao-Rico S**, **Librado P**, **Ramos-Onsins S**, **Sánchez-Gracia A. 2017.** DnaSP 6: DNA sequence polymorphism analysis of large datasets. *Molecular Biology and Evolution* **34:** 3299–3302.

Salzburger W, **Ewing G**, **von Haeseler A. 2011.** The performance of phylogenetic algorithms in estimating haplotype genealogies with migration. *Molecular Ecology* **20:** 1952–1963.

Sanjuán A, **De Carlos A**, **Rodríguez-Cabello C**, **Bañón R**, **Sánchez F**, **Serrano A. 2012.** Molecular identification of the arrowhead dogfish *Deania profundorum* (Centrophoridae) from the northern waters of the Iberian peninsula. *Marine Biology Research* **8:** 901–905.

Sarkar IN, **Planet PJ**, **DeSalle R. 2008.** CAOS software for use in character-based DNA barcoding. *Molecular Ecology Resources* **8:** 1256–1259.

Scacco U, **Mesa GL**, **Vacchi M. 2010.** Body morphometrics, swimming diversity and niche in demersal sharks: a comparative case study from the Mediterranean Sea. *Scientia Marina* **74:** 37–53.

Schmieder DA, **Benítez HA**, **Borissov IM**, **Fruciano C. 2015.** Bat species comparisons based on external morphology: a test of traditional versus geometric morphometric approaches. *PLoS One* **10:** e0127043.

Serena F. 2005. *Field identification guide to the sharks and rays of the Mediterranean and Black Sea*. Rome: Food and Agriculture Organization of the United Nations.

Serena F, **Abella AJ**, **Bargnesi F**, **Barone M**, **Colloca F**, **Ferretti F**, **Fiorentino F**, **Jenrette J**, **Moro S. 2020.** Species diversity, taxonomy and distribution of Chondrichthyes in the Mediterranean and Black Sea. *The European Zoological Journal* **87:** 497–536.

Simpfendorfer CA, **Kyne PM. 2009.** Limited potential to recover from overfishing raises concerns for deep-sea sharks, rays and chimaeras. *Environmental Conservation* **36:** 97–103.

Sternes PC, **Shimada K. 2020.** Body forms in sharks (Chondrichthyes: Elasmobranchii) and their functional, ecological, and evolutionary implications. *Zoology* **140:** 125799.

Straube N, **Iglesias SP**, **Sellos DY**, **Kriwet J**, **Schliewen UK. 2010.** Molecular phylogeny and node time estimation of bioluminescent Lantern Sharks (Elasmobranchii: Etmopteridae). *Molecular Phylogenetics and Evolution* **56:** 905–917.

Straube N, **White WT**, **Ho H-C**, **Rochel E**, **Corrigan S**, **Li C**, **Naylor GJP. 2013.** A DNA sequence-based identification checklist for Taiwanese chondrichthyans. *Zootaxa* **3752:** 256–278.

Swofford DL. 2002. *PAUP: phylogenetic analysis using parsimony (and other methods), v.4.0 beta 10*. Sunderland: Sinauer Associates,.

Tamura K, **Nei M. 1993.** Estimation of the number of nucleotide substitutions in the control region of mitochondrial DNA in humans and chimpanzees. *Molecular Biology and Evolution* **10:** 512–526.

Thompson JD, **Higgins DG**, **Gibson TJ. 1994.** CLUSTAL W: improving the sensitivity of progressive multiple sequence alignment through sequence weighting, position-specific gap penalties and weight matrix choice. *Nucleic Acids Research* **22:** 4673–4680.

Thomson KS. 1976. On the heterocercal tail in sharks. *Paleobiology* **2:** 19–38.

Thomson KS, **Simanek DE. 1977.** Body form and locomotion in sharks. *Integrative and Comparative Biology* **17:** 343–354.

Tudela S. 2004. *Ecosystem effects of fishing in the Mediterranean: an analysis of the major threats of fishing gear and practices to biodiversity and marine habitats. Studies and reviews*. Rome: General Fisheries Commission for the Mediterranean. FAO No. 74, 44.

Vargheese S, **Chowdhury LM**, **Ameri S**, **Anjela MA**, **Kathirvelpandian A. 2019.** Character based identification system for elasmobranchs for conservation and forensic applications. *Mitochondrial DNA Part A, DNA Mapping, Sequencing, and Analysis* **30:** 651–656.

Vella A, **Vella N**, **Schembri S. 2017.** A molecular approach towards taxonomic identification of elasmobranch species from Maltese fisheries landings. *Marine Genomics* **36:** 17–23.

Ventura D, **Bonhomme V**, **Colangelo P**, **Bonifazi A**, **Jona Lasinio G**, **Ardizzone G. 2017.** Does morphology predict trophic niche differentiation? Relationship between feeding habits and body shape in four co-occurring juvenile species (Pisces: Perciformes, Sparidae). *Estuarine, Coastal and Shelf Science* **191:** 84–95.

Veríssimo A, **McDowell JR**, **Graves JE. 2012.** Genetic population structure and connectivity in a commercially exploited and wide-ranging deepwater shark, the leafscale gulper (*Centrophorus squamosus*). *Marine and Freshwater Research* **63:** 505–512.

Veríssimo A, **Cotton CF**, **Buch RH**, **Guallart J**, **Burgess GH. 2014.** Species diversity of the deep-water gulper sharks (Squaliformes: Centrophoridae: *Centrophorus*) in North Atlantic waters – current status and taxonomic issues. *Zoological Journal of the Linnean Society* **172:** 803–830.

Ward RD, **Zemlak TS**, **Innes BH**, **Last PR**, **Hebert PDN. 2005.** DNA barcoding Australia's fish species. *Philosophical Transactions of the Royal Society B: Biological Sciences* **360:** 1847–1857.

Ward RD, **Holmes BH**, **White WT**, **Last PR. 2008.** DNA barcoding Australasian chondrichthyans: results and potential uses in conservation. *Marine and Freshwater Research* **59:** 57–71.

Watson R, **Kitchingman A**, **Gelchu A**, **Pauly D. 2004.** Mapping global fisheries: sharpening our focus. *Fish and Fisheries* **5:** 168–177.

White WT, **Last PR. 2012.** A review of the taxonomy of chondrichthyan fishes: a modern perspective. *Journal of Fish Biology* **80:** 901–917.

White WT, **Ebert DA**, **Naylor GJP**, **Ho H-C**, **Clerkin P**, **Veríssimo A**, **Cotton CF. 2013.** Revision of the genus *Centrophorus* (Squaliformes: Centrophoridae): Part 1 – Redescription of *Centrophorus granulosus* (Bloch & Schneider), a senior synonym of *C. acus* Garman and *C. niaukang* Teng. *Zootaxa* **3752:** 35–72.

White WT, **Ebert DA**, **Naylor GJP. 2017.** Revision of the genus *Centrophorus* (Squaliformes: Centrophoridae): Part 2 – Description of two new species of *Centrophorus* and clarification of the status of *Centrophorus lusitanicus* (Barbosa du Bocage & de Brito Capello, 1864). *Zootaxa* **4344:** 86–114.

Wienerroither RM, **Bjelland O**, **Bachmann L**, **Junge C. 2015.** Northernmost record of the little gulper shark *Centrophorus uyato* in the north-eastern Atlantic Ocean, with taxonomical notes on *Centrophorus zeehaani*. *Journal of Fish Biology* **86:** 834–844.

Wilke A, **Christe R**, **Multini L**, **Vidal P**, **Wilk R**, **Carvalho G**, **Marrelli M. 2016.** Morphometric wing characters as a tool for mosquito identification. *PLoS One* **11:** 8.

Wilga CD, **Lauder GV. 2002.** Function of the heterocercal tail in sharks: quantitative wake dynamics during steady horizontal swimming and vertical maneuvering. *Journal of Experimental Biology* **205:** 2365–2374.

Wilson AB, **Wegmann A**, **Ahnesjö I**, **Gonçalves JMS. 2020.** The evolution of ecological specialization across the range of a broadly distributed marine species. *Evolution* **74:** 629–643.

Wong EH, **Shivji MS**, **Hanner RH. 2009.** Identifying sharks with DNA barcodes: assessing the utility of a nucleotide diagnostic approach. *Molecular Ecology Resources* **9**(Suppl. s1): 243–256.

Yahn SN, **Baird RW**, **Mahaffy SD**, **Webster DL. 2019.** How to tell them apart? Discriminating tropical blackfish species using fin and body measurements from photographs taken at sea. *Marine Mammal Science* **35:** 1232–1252.

SUPPORTING INFORMATION

Additional Supporting Information may be found in the online version of this article at the publisher's web-site.

Figure S1. Scheme of the morphometric measurements taken from each specimen. Nomenclature and abbreviations defined according to Veríssimo *et al.* (2014) are here reported: TL, total length; FL, fork length; PD2, pre-second dorsal fin length; PD1, pre-first dorsal fin length; PG1, prebranchial length; IDS*, interdorsal space; DCS, dorsal-caudal fin space; CDM, dorsal caudal fin margin; PCA, pelvic fin caudal fin space; CPV, preventral caudal fin margin; HDL, head length; PP2, prepelvic fin length; PN, prenarial length; POR, preoral length; D1A, first dorsal fin anterior margin; D1B, first dorsal fin base; D1B', first dorsal fin base, from the posterior insertion of the spine; D1H, first dorsal fin height; D1I, first dorsal fin inner margin; D2A, second dorsal fin anterior margin; D2B, second dorsal fin base; D2B', second dorsal fin base, from the posterior insertion of the spine; D2H, second dorsal fin height; D2I, second dorsal fin inner margin; P1A, pectoral fin anterior margin; P1B, pectoral fin base; P1H, pectoral fin height; P1I, pectoral fin inner margin. * following Verissimo *et al*. 2014 where IDS is defined as 'distance from first dorsal fin insertion to second dorsal fin insertion'.

Figure S2. A, positions of the seven caudal fin landmarks (lmk):.lmk 1, caudal fin upper origin; lmk 2, posterior tip; lmk 3, posterior tip of subterminal margin; lmk 4, subterminal notch; lmk 5, deepest point of the caudal fork; lmk 6, ventral tip; lmk 7, caudal fin lower origin. B, positions of the five dorsal fin landmarks (lmk): lmk 1, fin origin; lmk 2, fin spine insertion; lmk 3, fin tip; lmk 4, end of the free rear tip; lmk 5, fin insertion.

Figure S3. The plot of the first two major axes of the principal coordinates analysis based on the K2P genetic distances.

Figure S4. Maximum likelihood phylogenetic tree of the *COI* haplotypes. Near the nodes are the support values, shown as bootstrap values > 50. In red the haplotypes from individuals sequenced in the present study.

Figure S5. Neighbour-joining phylogenetic tree of the *COI* haplotypes. Near the nodes are the support values, shown as bootstrap values > 50. In red the haplotypes from individuals sequenced in the present study.

Figure S6. Maximum likelihood phylogenetic tree of the 16S haplotypes. Near the nodes are the support values, shown as bootstrap values > 50. In red the haplotypes from individuals sequenced in the present study.

Figure S7. Neighbour-joining phylogenetic tree of the 16S haplotypes. Near the nodes are the support values, shown as bootstrap values > 50. In red the haplotypes from individuals sequenced in the present study.

Figure S8. Maximum likelihood phylogenetic tree of the *ND2* haplotypes. Near the nodes are the support values, shown as bootstrap values > 50. In red the haplotypes from individuals sequenced in the present study.

Figure S9. Neighbour-joining phylogenetic tree of the *ND2* haplotypes. Near the nodes are the support values, shown as bootstrap values > 50. In red the haplotypes from individuals sequenced in the present study.

Figure S10. Analysis of principal coordinates (CAP) scatterplot representing the morphometric differences observed among the species resulted from the genetic analyses, including 49 Mediterranean individuals without molecular identification, assumed to be *Centrophorus* cf. *uyato*. Specimens of *Centrophorus* cf. *uyato* collected in the Atlantic Ocean are circled in red.

Figure S11. Principal component analysis (PCA) conducted on caudal fin (A), first dorsal fin (B) and second dorsal fin (C) landmarks of *Centrophorus* cf *uyato*. Light blue dots correspond to male individuals and pink dots correspond to female individuals.

Figure S12. Canonical variates analysis (CVA) performed on caudal fin (A), first dorsal fin (B) and second dorsal fin (C) landmarks. Blue, pink and red dots represent, respectively, *Centrophorus* cf. *uyato*, *Centrophorus granulosus* and *Centrophorus squamosus* samples.

Figure S13. Relationship between centroid size and total length (TL) for the caudal fin (A), first dorsal fin (B) and second dorsal fin (C) of *Centrophorus* cf. *uyato* specimens. Males and females are represented, respectively, in light blue and pink.

Figure S14. Relationship between shape (Procrustes coordinates) and total length (TL) for the caudal fin (A), first dorsal fin (B) and second dorsal fin (C) of *Centrophorus* cf. *uyato* specimens. Male and female specimens correspond, respectively, to light blue and pink dots.
Table S1. Details of specimens analysed in this study: sampling, morphological and genetic data are reported in detail for each individual.
Table S2. Details of the *COI* sequences mined from GenBank and or BOLD. Clade as in Figure 4. *COI* Haps = *COI* haplotype, Molecular assigned species, Original attribution, BOLD ID, Voucher, GenBank ID, BIN, Location, Area, other = localities other than the voucher, Reference.
Table S3. Details of the 16S sequences mined from GenBank and or BOLD. Clade as in Figure 5. 16S Haps = 16S haplotype, Molecular assigned species, Original attribution, BOLD ID, Voucher, GenBank ID, Location, Area, other = localities other than the voucher, Reference.
Table S4. Details of the *ND2* sequences mined from GenBank and or BOLD. Clade as in Figure 6. *ND2* Haps = *ND2* haplotype, Molecular assigned species, Original attribution, BOLD ID, Voucher, GenBank ID, Location, Area, other = localities other than the voucher, Reference.
Table S5. Details of the sequences analysed in this study: Clade as in Figures 4-6, *COI* Haps = *COI* haplotype, GenBank *COI* ID, *ND2* Haps= *ND2* haplotype, GenBank *ND2* ID, 16S Haps = 16S haplotype, GenBank 16S ID, Concatenated haplotype, molecular assigned species, morphological assigned species, Voucher, BOLD ID, BIN, Location, Area, Reference.
Table S6. Character-based DNA sequences for *C.* cf. *uyato*, *C. squamosus* and *C. granulosus* showing the diagnostic character states in the 28S, 16S, *COI* and *ND2* gene sequences, respectively. Combinations of character states at specific nucleotide positions are diagnostic for clades' identification. Black cells represent transversion events and transitions are also reported.
Table S7. Character-based DNA sequences for 8, 14 and 15 clades retrieved from 16S, *COI* and *ND2* genes, respectively. Combinations of character states at specific nucleotide positions are diagnostic for clades' identification. Grey cells highlight the lack of diagnostic character (DC), while black cells represent transversion events. Transitions are also reported.
Table S8. Species-specific range of morphometric measurements reported in percentage of total length (TL). *N* represents the number of individuals considered for the analyses. Refer to Figure S1 for measurements' acronyms.
Table S9. Cross-validation of the CAP analysis performed among the three groups of gulper shark genetically identified. Percentages of samples correctly allocated to each group, total correct assignment and mis-classification error are also reported.
Table S10. SIMPER analysis results showing the contribution of each measurement to the intraspecific similarity and pairwise dissimilarity between *C.* cf. *uyato*, *C. squamosus*, *C. granulosus*. Cumulative and punctual average values of similarity are provided for each measurement considered. Refer to Figure S1 for measurements' acronyms.
Table S11. Discriminant function analysis results showing the number of samples correctly and incorrectly assigned to each group in the pairwise comparison. The total number of samples analysed is also reported.
Text S1. Details of amplification conditions for *COI*, *ND2*, 16S and 28S markers.